Multi-Target Effects of the Cannabinoid CP55940 on Familial Alzheimer's Disease PSEN1 E280A Cholinergic-Like Neurons: Role of CB$_1$ Receptor

Viviana Soto-Mercado, Miguel Mendivil-Perez, Marlene Jimenez-Del-Rio* and Carlos Velez-Pardo*
Neuroscience Research Group, Medical Research Institute, Faculty of Medicine, University of Antioquia (UdeA), SIU Medellin, Colombia

Abstract.

Background: Alzheimer's disease (AD) is characterized by structural damage, death, and functional disruption of cholinergic neurons (ChNs) as a result of intracellular amyloid-β (Aβ) aggregation, extracellular neuritic plaques, and hyperphosphorylation of protein tau (p-Tau) overtime.

Objective: To evaluate the effect of the synthetic cannabinoid CP55940 (CP) on PSEN1 E280A cholinergic-like nerve cells (PSEN1 ChLNs)—a natural model of familial AD.

Methods: Wild type (WT) and PSEN1 ChLNs were exposed to CP (1 μM) only or in the presence of the CB$_1$ and CB$_2$ receptors (CB$_1$Rs, CB$_2$Rs) inverse agonist SR141716 (1 μM) and SR144528 (1 μM) respectively, for 24 h. Untreated or treated neurons were assessed for biochemical and functional analysis.

Results: CP in the presence of both inverse agonists (hereafter SR) almost completely inhibits the aggregation of intracellular sAβPPβf and p-Tau, increases $\Delta\Psi_m$, decreases oxidation of DJ-1Cys^{106}-SH residue, and blocks the activation of c-Jun, p53, PUMA, and caspase-3 independently of CB$_1$Rs signaling in mutant ChLNs. CP also inhibits the generation of reactive oxygen species partially dependent on CB$_1$Rs. Although CP reduced extracellular Aβ$_{42}$, it was unable to reverse the Ca^{2+} influx dysregulation as a response to acetylcholine stimuli in mutant ChLNs. Exposure to anti-Aβ antibody 6E10 (1:300) in the absence or presence of SR plus CP completely recovered transient [Ca^{2+}]$_i$ signal as a response to acetylcholine in mutant ChLNs.

Conclusion: Taken together our findings suggest that the combination of cannabinoids, CB$_1$Rs inverse agonists, and anti-Aβ antibodies might be a promising therapeutic approach for the treatment of familial AD.

Keywords: Apoptosis, cannabinoids, cholinergic neurons, CP55940, E280A mutation, familial Alzheimer disease, neuronal dysfunction, oxidative stress, PSEN1, sAβPPβf, tau

INTRODUCTION

Alzheimer's disease (AD) is a multifactorial neurodegenerative condition [1] characterized by severe loss of cholinergic neurons from the nucleus basalis magnocellularis of Meynert and cholinergic projections to the cortex and hippocampus [2]. The neuronal destruction is associated with the extracellular accumulation of insoluble forms of amyloid-β (Aβ) in plaques, mostly fragment Aβ$_{1-42}$ (hereafter

*Correspondence to: Carlos Velez-Pardo and Marlene Jimenez-Del-Rio, Neuroscience Research Group, Medical Research Institute, Faculty of Medicine, University of Antioquia (UdeA), Calle 70 No. 52-21, and Calle 62 # 52-59, Building 1, Room 412; SIU Medellin, Colombia. E-mail: calberto.velez@udea.edu.co., ORCID #0000-0002-0557-0411 (Velez-Pardo); E-mail: marlene.jimenez@udea.edu.co., ORCID #0000-0003-3477-2386 (Jimenez-Del-Rio)

$A\beta_{42}$), intracellular aggregation of the microtubule protein tau in neurofibrillary tangles, neuronal cell death, and synaptic dysfunction [3]. The $A\beta_{42}$ peptide is derived from the amyloid-β protein precursor (AβPP) via sequential cleavage by the beta-site amyloid precursor protein cleaving enzyme 1 (BACE1) and by the gamma-site aspartyl protease γ-secretase [4]. This last protein is composed of four subunits, namely presenilins (PSEN1 and PSEN2), presenilin enhancer 2 (PEN2), anterior pharynx-defective 1 (APH-1), and nicastrin. While PEN2, APH-1, and nicastrin stabilize the complex, PSEN1 and PSEN2 function as the catalytic core of the protease [5]. Over two hundred autosomal dominant mutations in the presenilin 1 (*PSEN 1*) gene result in the overproduction of extracellular (e)$A\beta_{42}$ [6] and occur most frequently in familial AD (FAD; https://www.alzforum.org/mutations/psen-1). Among PSEN1 mutations, the Glu280Ala (p. E280A, c.839A>C, exon 8) in *PSEN1* causes FAD with complete penetrance in a large kindred localized in Antioquia, Colombia [7–10]. As the majority of dominant-negative *PSEN1* mutations [11], PSEN1 E280A produces increased $A\beta_{42}$ deposition [12], hippocampal neuron loss [13], and Aβ/tau accumulation in young adults [14, 15]. Recently, we have recapitulated the molecular pathogenesis of FAD caused by PSEN1 E280A in umbilical cord mesenchymal stem cells-derived cholinergic-like neurons (ChLNs [16]). It has demonstrated that PSEN1 E280A ChLNs effectively exhibited not only an increased e$A\beta_{42}$ but also an early increased of intracellular sAβPPβ fragments (but not $A\beta_{42}$ peptide) and tau phosphorylation. Moreover, PSEN1 E280A ChLNs exhibited oxidized DJ-1 (at $Cys^{106}SO_3$) indicative of oxidative stress (OS), and concomitant loss of the mitochondrial membrane potential ($\Delta\Psi_m$), activation of apoptogenic proteins, and DNA fragmentation, markers of apoptosis—a type of regulated cell death. Additionally, mutant ChLNs displayed Ca^{2+} flux dysregulation when challenged to acetylcholine (ACh) and deficient acetylcholinesterase (AChE) activity compared to wild type (WT) ChLNs most probably due to e$A\beta_{42}$ peptide. Taken together these observations suggest that PSEN1 E280A ChLNs display the typical neuropathological markers of AD; therefore, mutant ChLNs provide a unique FAD model for screening of candidate molecule(s)/drug(s).

Due to the lack of effective therapies to date for AD, the need for new drugs has become increasingly urgent. Phytocannabinoids, a group of biologically active compounds isolated from the plant *Cannabis sativa* [17], have been postulated to possess therapeutic potential for clinical purposes in AD [18]. *Cannabis* contains at least 120 kinds of cannabinoids mainly classified as Δ^9-trans-tetrahydrocannabidiol (THC), cannabidiol (CBD), CBG (Cannabigerol), and CBN (Cannabinol), among others [19]. Biologically, cannabinoids, endocannabinoids (e.g., anandamide, 2-arachidonoylglycerol), and synthetic cannabimimetic compounds (e.g., CP55940) bind cannabinoid type 1 and 2 receptors (CB_1R/ CB_2R), two G-protein-coupled receptors (GPCR) [20, 21]. Interestingly, it has been shown *in vitro* that 9 out of 11 cannabinoids studied, including THC, were able to protect cells (e.g., MC65—a human neuron-like cell line, HT22 mouse hippocampal nerve cell line, primary cortical neurons from 18-day-old rat embryos, BV2—a microglial cell line) in four distinct phenotypic neurodegeneration screening assays including proteotoxicity, loss of trophic support, OS, energy loss, and inflammation [22]. Outstandingly, cannabinoids were able to remove intraneuronal Aβ, reduce oxidative damage, and protect from the loss of energy or trophic support in neurons in which CB_1 and CB_2 receptors were lacking (e.g., MC65 and HT22 cells). Furthermore, CB_1 agonists (e.g., CP55940) were also effective neuroprotective agents against Aβ toxicity in MC65 neurons [22]. These data suggest that cannabinoids might be antioxidant and anti-amylogenic compounds through receptor-independent mechanisms in a cell- and species-specific manner [22–28]. Despite these observations, no data are available to establish whether cannabinoids might reverse the neuropathological markers, i.e., intracellular sAβPPβf aggregation, hyperphosphorylation of tau protein, and DJ-1 oxidation in PSEN1 E280A ChLNs. Furthermore, it is not yet known whether cannabinoids might be able to block neuronal apoptosis, e$A\beta_{42}$, and/or prevent Ca^{2+} dysregulation in those mutant cholinergic neurons.

To get insight into these issues, we have selected the commercially available CP55940 ((-)-cis-3-[2-Hydroxy-4-(1,1-dimethylheptyl)phenyl]-trans-4-(3-hydroxypropyl)cyclohexanol, hereafter CP), a CB_1 and CB_2 potent bicyclic analog of THC [29], to evaluate its effect on wild-type and PSEN1 E280A ChLNs concerning the intracellular sAβPPβf accumulation, tau phosphorylation, OS, cell death, and Ca^{2+} neuronal dysfunction in ChLNs. We demonstrate for the first time that CP can protect FAD PSEN1 E280A ChLNs against neuronal structural

damage and OS-induced cell death signaling and that it can reverse the cholinergic dysfunction in the presence of eAβ_{42} blocking agents (e.g., anti-Aβ_{42} antibody 6E10). These findings might favor the use of cannabinoids as potential lead compound candidates as a combined therapy for FAD.

MATERIALS AND METHODS

Cholinergic-like neuron (ChLN) differentiation

ChLN differentiation was performed according to [30]. The WT (TBC# WJMSC-11) and PSEN1 E280A (TBC# WJMSC-12) [16] MSCs were seeded at $1-1.5 \times 10^4$ cells/cm^2 in laminin-treated culture plates for 24 h in regular culture medium (*RCm*). Then, the medium was removed, and cells were incubated in cholinergic differentiation medium (*Cholinergic-N-Run medium*, hereafter *Ch-N-Rm*) containing DMEM/F-12 media 1:1 Nutrient Mixture (Gibco cat# 10565018), 10 ng/ mL basic fibroblast growth factor (bFGF) recombinant human protein (Gibco Cat# 13256029), 50 μg/ mL sodium heparin (Hep, Sigma-Aldrich cat# H3393), 0.5 μM all-trans retinoic acid, 50 ng/ml sonic hedgehog peptide (SHH, Sigma cat# SRP3156) and 1% FBS at 37°C for 7 days. After this process of transdifferentiation, the cells were labeled as WT PSEN1 or PSEN1 E280A ChLNs. Since *Ch-N-Rm* contains several factors that might interfere with the experiment interpretation and measurements, WT PSEN1 and PSEN1 E280A ChLNs (obtained after 7 days in *Ch-N-Rm*) were left in regular culture medium (*RCm*) for 4 additional days of post transdifferentiation.

Immunofluorescence analysis

For the analysis of markers of AD, oxidative stress, and cell death, the cells treated under different conditions were fixed with 4% paraformaldehyde for 20 min, followed by Triton X-100 (0.1%) permeabilization and 10% bovine serum albumin (BSA) blockage. Cells were incubated overnight with primary antibodies against APP$_{751}$ and/or protein amyloid β_{1-42} (1:500; clone 6E10 cat# 803014, Biolegend), total tau (1:500; t-Tau; cat# T6402, Sigma), and phospho-tau (p-Tau, 1:500, Ser202/ Thr205, cat# MN1020 (AT8), Thermo Fisher Scientific); and primary antibodies against oxidized DJ-1 (1:500; ox(Cys106)DJ-1; spanning residue C^{106} of human PARK7/DJ1; oxidized to produce cysteine sulfonic (SO$_3$) acid; cat # ab169520, Abcam). To assess cell death, we used primary antibodies

against p53-upregulated modulator of apoptosis (1:500; PUMA, cat# ab-9643, Abcam), p53 (1:500; cat# MA5-12453, Millipore), phospho-c-Jun (1:250; c-Jun (S63/73) cat# sc-16312, Santa Cruz), and caspase-3 (1:250; cat # AB3623, Millipore). After exhaustive rinsing, we incubated the cells with secondary fluorescent antibodies (DyLight 488 and 594 horse anti-rabbit, -goat and -mouse, cat DI 1094, DI 3088, and DI 2488, respectively) at 1:500. The nuclei were stained with 1 μM Hoechst 33342 (Life Technologies), and images were acquired on a Floyd Cells Imaging Station microscope.

Western blot analysis

Cells were incubated as described above, detached with 0.25% trypsin and lysed in 50 mM Tris-HCl, pH 8.0, with 150 mM sodium chloride, 1.0% Igepal CA-630 (NP-40), and 0.1% sodium dodecyl sulfate and a protease inhibitor cocktail (Sigma-Aldrich). All lysates were quantified using the bicinchoninic acid assay (Thermo Scientific cat # 23225). Extracted samples (30 μg of proteins) were heated at 95°C for 5 min in $2 \times$ SDS and $20\times$ reducing agent (except for protein oxDJ-1) and loaded on to 12% gels at 120 V for 90 min, and the bands were transferred onto nitrocellulose membranes (Hybond-ECL, Amersham Biosciences) at 270 mA for 90 min using an electrophoretic transfer system (BIO-RAD) according to Bio-Rad protocol (http://www.bio-rad.com/webroot/ web/pdf/lsr/literature/Bulletin_6376). The membranes were incubated overnight at 4°C with anti-APP$_{751}$, total tau, phospho-Tau, ox(Cys^{106}) DJ1, PUMA, p53, p-c-Jun, and caspase-3 primary antibodies (1:5000). The anti-actin antibody (1:1000, cat #MAB1501, Millipore) was used as an expression control. Secondary infrared antibodies (goat anti-rabbit IRDye® 680 RD, cat #926-68071; donkey anti-goat IRDye ® 680 RD, cat # 926-68074; and goat anti-mouse IRDye ® 800 CW, cat #926-32270; LI-CORBiosciences) at 1:1000 were used for western blotting analysis, and data were acquired using Odyssey software. The determination of the aggregation state of APP$_{751}$ (i.e., sAβPPβf) was performed by western analysis of SDS-PAGE as described above. The assessment was repeated three times in independent experiments.

Analysis of cells

Assay protocol

The methodology for both WT and PSEN1 E280A ChLNs cell culture assays was the same. Initial

CP55940 screening was performed at least twice in triplicate between 10 nM and 1 μM. Subsequently, CP55940 (1 μM) was established as an optimal concentration for further experiments. ChLNs were divided in four groups: 1) untreated; 2) treated with SR141716 (CB_1 receptor inverse agonist) and SR144528 (CB_2 receptor inverse agonist) at 1 μM final concentration each (hereafter SR); 3) CP55940 (or CP); 4) RS + CP55940 (also named as SR + CP cocktail). To block $eA\beta_{42}$ [31], WT and mutant ChLNs were incubated four days with anti-$A\beta_{42}$ antibody 6E10 (1:300 in *RCm*) after differentiation in the presence or absence of CP or CP + RS.

Evaluation of intracellular hydrogen peroxide (H_2O_2) by fluorescence microscopy

To determine the levels of intracellular H_2O_2, we used $2',7'$-dichlorofluorescein diacetate (5 μM, DCFH2-DA; Invitrogen). ChLNs were left in RCm for 4 days. Then, the cells (5×10^3) were incubated with the DCFH$_2$-DA reagent for 30 min at 37°C in the dark. Cells were then washed, and DCF fluorescence intensity was determined by analysis of fluorescence microscopy images. The assessment was repeated three times in independent experiments. The nuclei were stained with 0.5 μM Hoechst 33342 staining compound. The assessment was repeated three times in independent experiments blind to the experimenter.

Analysis of mitochondrial membrane potential ($\Delta\Psi m$) by fluorescence microscopy

The ChLNs were left in regular culture medium (*RCm*) for 4 days. Then, the cells (5×10^3) were incubated with the passively diffusing and active mitochondria-accumulating dye deep red Mito-Tracker compound (20 nM, final concentration) for 20 min at room temperature in the dark (Invitrogen, cat # M22426). Cells were then washed twice with PBS. MitoTracker fluorescence intensity was determined by analysis of fluorescence microscopy images. The assessment was repeated three times in independent experiments. The nuclei were stained with 0.5 μM Hoechst 33342 staining compound. The assessment was repeated three times in independent experiments blind to the experimenter and flow cytometer analyst.

Measurement of $A\beta_{42}$ peptide in culture medium

The level of $A\beta_{1-42}$ peptide was measured according to a previous report [32] with minor modifications. Briefly, WT and PSEN1 E280A ChLNs were left in *RCm* for 4 days. Then, 100 μl of con-ditioned medium was collected, and the levels of secreted $A\beta_{42}$ peptides were determined by a solid-phase sandwich ELISA (Invitrogen, Cat# KHB3544) following the manufacturer's instructions. The assessment was repeated 4 times in independent experiments blind to the experimenter.

Intracellular calcium imaging

Intracellular calcium (Ca^{2+}) concentration changes evoked by cholinergic stimulation were assessed according to [33, 34] with minor modifications. For the measurement, the fluorescent dye Fluo-3 (Fluo-3 AM; Thermo Fisher Scientific, cat: F1242) was employed. The dye was dissolved in DMSO (1 mM) to form a stock solution. Before the experiments, the stock solution was diluted in neuronal buffer solution (NBS buffer: 137 mM NaCl, 5 mM KCl, 2.5 mM $CaCl_2$, 1 mM $MgCl_2$, pH 7.3, and 22 mM glucose). The working concentration of the dye was 2 μM. The WT and PSEN1 E280A ChLNs were incubated for 30 min at 37°C with the dye-containing NBS and then washed five times. Intracellular Ca^{2+} transients were evoked by acetylcholine (1 mM final concentration) at 4 days post differentiation. The measurements were carried out using the 20× objective of the microscope. Several regions of interest (ROIs) were defined in the visual field of the camera. One of the ROIs was cell-free, and the fluorescence intensity measured here was considered background fluorescence (F_{bg}). The time dependence of the fluorescence emission was acquired, and the fluorescence intensities (hence the Ca^{2+} levels) were represented by pseudo colors. To calculate the changes of the average Ca^{2+}-related fluorescence intensities, the F_{bg} value was determined from the cell-free ROI, and then the resting fluorescence intensities (F_{rest}) of the cell-containing ROIs were obtained as the average of the points recorded during a consecutive period of 10 s before the addition of acetylcholine. The peaks of the fluorescence transients were found by calculating the average of six consecutive points and identifying those points that gave the highest average value (F_{max}). The amplitudes of the Ca^{2+}-related fluorescence transients were expressed relative to the resting fluorescence ($\Delta F/F$) and were calculated by the following formula: $\Delta F/F = (F_{max}-F_{rest})/(F_{rest}-F_{bg})$. For the calculation of the fluorescence intensities, ImageJ was used. The terms fluorescence intensity was used as an indirect indicator of intracellular Ca^{2+} concentration. The assessment was repeated three times in independent experiments blind to the experimenter.

Photomicrography and image analysis

Light microscopy photographs were taken using a Zeiss Axiostart 50 Fluorescence Microscope equipped with a Canon PowerShot G5 digital camera (Zeiss Wöhlk-Contact-Linsen, Gmb Schcönkirchen, Germany), and fluorescence microscopy photographs were taken using a Zeiss Axiostart 50 Fluorescence Microscope equipped with a Zeiss AxioCam Cm1 and (Zeiss Wöhlk-Contact-Linsfluoreen, Gmb Schcönkirchen, Germany) and Floyd Cells Imaging Station microscope. Fluorescence images were analyzed by ImageJ software (http://imagej.nih.gov/ij/). The figures were transformed into 8-bit images, and the background was subtracted. The cellular measurement ROIs were drawn around the nucleus (for the case of transcription factors and apoptosis effectors) or overall cells (for cytoplasmic probes), and the fluorescence intensity was subsequently determined by applying the same the threshold for cells in the control and treatment conditions. Mean fluorescence intensity (MFI) was obtained by normalizing total fluorescence to the number of nuclei.

Data analysis

In this experimental design, a vial of MSCs was thawed, cultured and the cell suspension was pipetted at a standardized cellular density of 2.6×10^4 cells/ cm^2 into different wells of a 24-well plate. Cells (i.e., the biological and observational unit [35]) were randomized to wells by simple randomization (sampling without replacement method), and then wells (i.e., the experimental units) were randomized to treatments by a similar method. Experiments were conducted in triplicate wells. The data from individual replicate wells were averaged to yield a value of $n = 1$ for that experiment and this was repeated on three occasions blind to the experimenter and/ or flow cytometer analyst for a final value of $n = 3$ [35]. Based on the assumption that the experimental unit (i.e., the well) data comply with the independence of observations, the dependent variable is normally distributed in each treatment group (Shapiro-Wilk test), and variances are homogeneous (Levene's test), the statistical significance was determined by one-way analysis of variance (ANOVA) followed by Tukey's *post hoc* comparison calculated with GraphPad Prism 5.0 software. Differences between groups were only deemed significant when a *p*-value of < 0.05 (*),< 0.001 (**) and < 0.001 (***). All data are illustrated as the mean $\pm$ S.D.

RESULTS

CP55940 restores the mitochondrial membrane potential ($\Delta\Psi_m$) and blunts generation of ROS in PSEN1 E280A ChLNs in an independent concentration fashion

Previously, it has been shown that PSEN 1 E280A ChLNs present aggregation of sAβPPβf, endogenously generated OS, and loss of $\Delta\Psi_m$ as the earliest neuropathological markers in mutant ChLNs [16]. Therefore, we initially determined whether CP could recover $\Delta\Psi_m$ and scavenge ROS in those cells. To this aim, cholinergic cells were exposed to increasing concentrations of CP. As shown in Fig. 1A'-E', CP did not affect $\Delta\Psi_m$ in wild type ChLNs (Fig. 1A–E, K). However, it significantly increased the $\Delta\Psi_m$ in PSEN1 E280A ChLNs in a concentration-independent fashion (Fig. 1F'-J'). Accordingly, we found 500 nM –1000 nM (= 1 μM), but not low concentrations (10, 100 nM), as the maximal optimal concentrations to raise $\Delta\Psi_m$ in mutant cells (Fig. 1F-J, K). Figure 1 shows mutant ChLNs (Fig. 1F") but no WT ChLNs (Fig. 1A") endogenously produce ROS. CP blunted ROS yield in mutant ChLNs (Fig. 1G"-J") compared to WT ChLNs (Fig. 1B"-E") in an independent concentration fashion. Since CP (1 μM) recovered $\Delta\Psi_m$ to control levels and completely diminished ROS in mutant ChLNs (Fig. 1K, L), we selected this concentration for further experiments.

CP55940 restores $\Delta\Psi_m$ in a CB$_1$ receptor-independent manner but diminishes ROS production partially dependent on CB$_1$ receptors in PSEN1 E280A ChLNs

We wanted to establish whether the neuroprotective effect on mitochondria and antioxidant activity of CP was due to interaction with CB$_1$Rs. Although these receptors are expressed in cholinergic neurons [36] and CP is a CB$_1$ and CB$_2$ receptor agonist, we used both potent and highly specific CB$_1$ and CB$_2$ receptor inverse agonist SR141716 and SR144528 (hereafter SR at 1 μM each) only or with CP agonist (i.e., SR + CP cocktail) to avoid ambiguous observations. Figure 2 shows that while SR only neither affects $\Delta\Psi_m$ in wild type ChLNs (i.e., high $\Delta\Psi_m$ Fig. 2C) nor in mutant ChLNs (i.e., low $\Delta\Psi_m$ Fig. 2D) when compared to untreated neurons
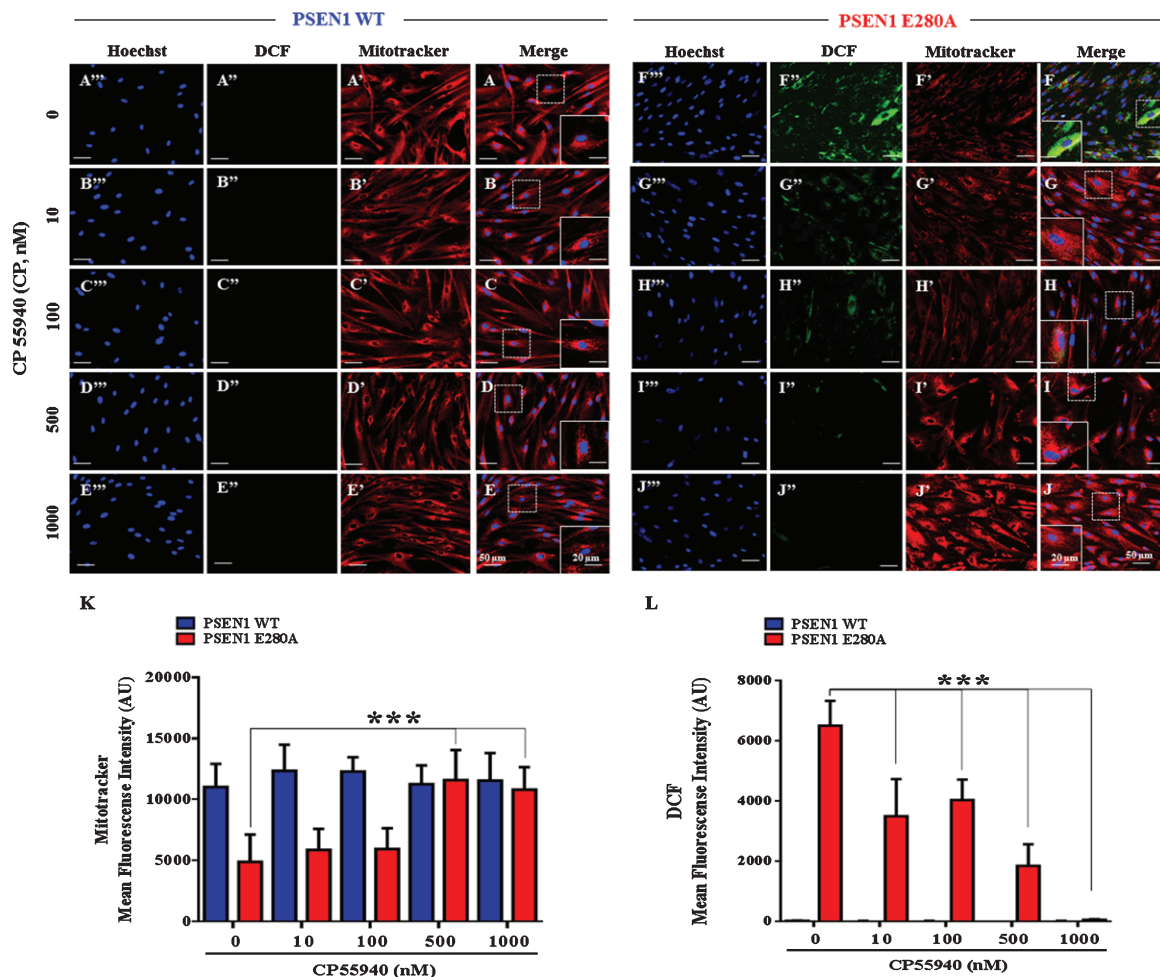
Fig. 1. CP55940 restores the mitochondrial membrane potential ($\Delta\Psi_m$) and reduces the levels of intracellular reactive oxygen species independent of its concentration in PSEN1 E280A ChLNs. After 7 days of transdifferentiation, WT PSEN1 and PSEN1 E280A ChLNs were left untreated or treated with CP at increasing concentrations (0, 10, 100, 500, and 1000 nM) in regular culture medium (RCm) for 4 days. Representative MitoTracker (A'-J'), DCF (A''-J''), Hoechst (A'''-J'''), and merge (A-J) pictures of WT PSEN1 and PSEN1 E280A ChLNs treated as described. K) Quantification of MitoTracker fluorescence intensity. L) Quantification of DCF fluorescence intensity. Data are expressed as the mean ± SD; *$p < 0.05$; **$p < 0.01$; ***$p < 0.001$. The histograms and figures represent 1 out of 3 independent experiments. Image magnification, 200×. Inset magnification, 800×.

(Fig. 2A, B), CP (Fig. 2F) or CP + SR (Fig. 2H) significantly increased the $\Delta\Psi_m$ in mutant ChLNs (Fig. 2I). Neither CP nor the cocktail altered $\Delta\Psi_m$ in WT ChLNs (Fig. 2E, G, I). However, analysis of ROS disappearance in ChLNs shows that while CP only almost completely scavenged ROS in mutant ChLNs (Fig. 2J), the SR + CP cocktail diminished ROS by almost half of the value of untreated or treated with SR only in PSEN1 E280A ChLNs (Fig. 2J). WT ChLNs produced no detectable ROS in any experimental condition (Fig. 2J). Of note, SR only treatment showed no effect in $\Delta\Psi_m$ and ROS conditions in both WT (Fig. 2I) and mutant ChLNs (Fig. 2J).

CP55940 reduces intracellular sAβPPβf aggregation in a CB$_1$Rs-independent fashion but it reduces oxidized DJ-1 partially dependent of CB$_1$Rs in PSEN1 E280A ChLNs

Next, we assessed whether CP could inhibit intracellular aggregation of sAβPPβf and avoid oxidation of the stress sensor protein DJ-1. To this aim, WT and mutant ChLNs were left untreated or exposed to CP in the absence or presence of SR. Western blot analysis revealed that CP only or with SR reduced the aggregation of sAβPPβf in a CB$_1$Rs-independent manner (Fig. 3A, B) but blunted the oxidation of
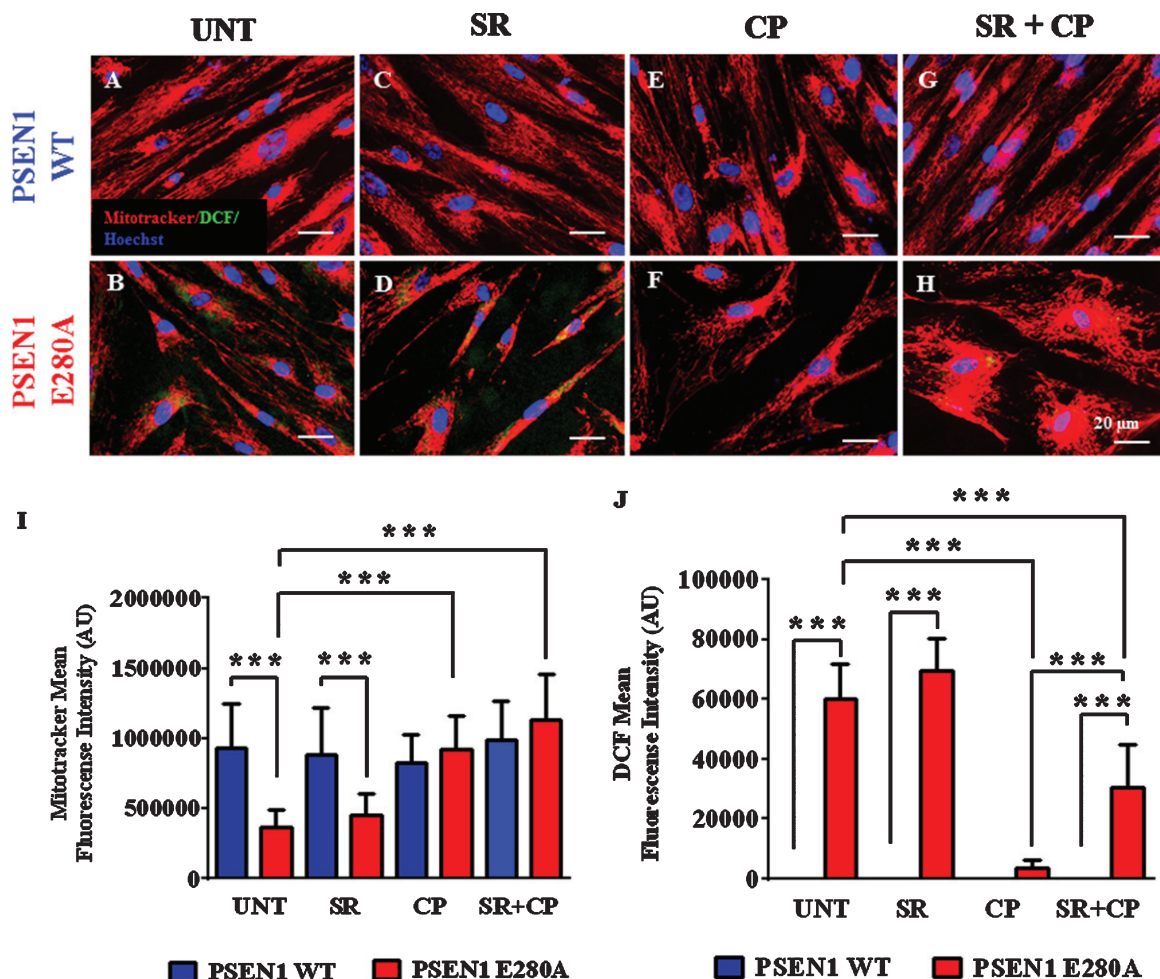
Fig. 2. CP55940 augments the Ψ_m independent of CB_1R but reduced the levels of intracellular reactive oxygen species partially dependent on those receptors in PSEN1 E280A ChLNs. After 7 days of transdifferentiation, WT PSEN1 and PSEN1 E280A ChLNs were left untreated or treated with SR, CP, or SR + CP in RCm for 4 days. A-H) Representative MitoTracker/DCF/Hoechst merge pictures of WT PSEN1 and PSEN1 E280A ChLNs treated as described. I) Quantification of MitoTracker fluorescence intensity. J) Quantification of DCF fluorescence intensity. Data are expressed as the mean ± SD; *$p < 0.05$; **$p < 0.01$; ***$p < 0.001$. The histograms and figures represent 1 out of 3 independent experiments. Image magnification, 400×.

DJ-1 partially dependent of CB_1Rs (Fig. 3A, C). As expected, WT ChLNs remained unaltered to CP and to the cocktail exposure. Neither sAβPPβf nor oxidized DJ-1 were detected in those neurons (Fig. 3A–C). These results were confirmed by fluorescent microscopy (Fig. 3D–M).

CP55940 blocks apoptosis in a CB₁Rs-independent manner in PSEN1 E280A ChLNs

Cell death by apoptosis is a prominent feature in mutant ChLNs [16]. We used, therefore, the activation of the transcription factors p53 and c-Jun,

pro-apoptotic BH3-only protein PUMA, and protease caspase-3 as apoptosis markers to examine the effect of CP and/or SR plus CP on those neuronal cells. Effectively, we confirmed that ChLNs displayed high levels of protein c-Jun (Fig. 4A, B), p53 (Fig. 4A, C), PUMA (Fig. 4A, D), and caspase-3 (Fig. 4A, E) in mutant but not in WT ChLNs (Fig. 4A–E). No significant difference was found between untreated and SR treatment for all the apoptosis markers in both types of cells. However, CP only or CP + SR significantly reduced c-Jun (Fig. 4A, B), p53 (Fig. 4A, C), PUMA (Fig. 4A, D), and caspase-3 (Fig. 4A, E) in PSEN1 E280A neurons when compared to untreated cells or WT ChLNs. Interestingly, mutant neurons exposed to
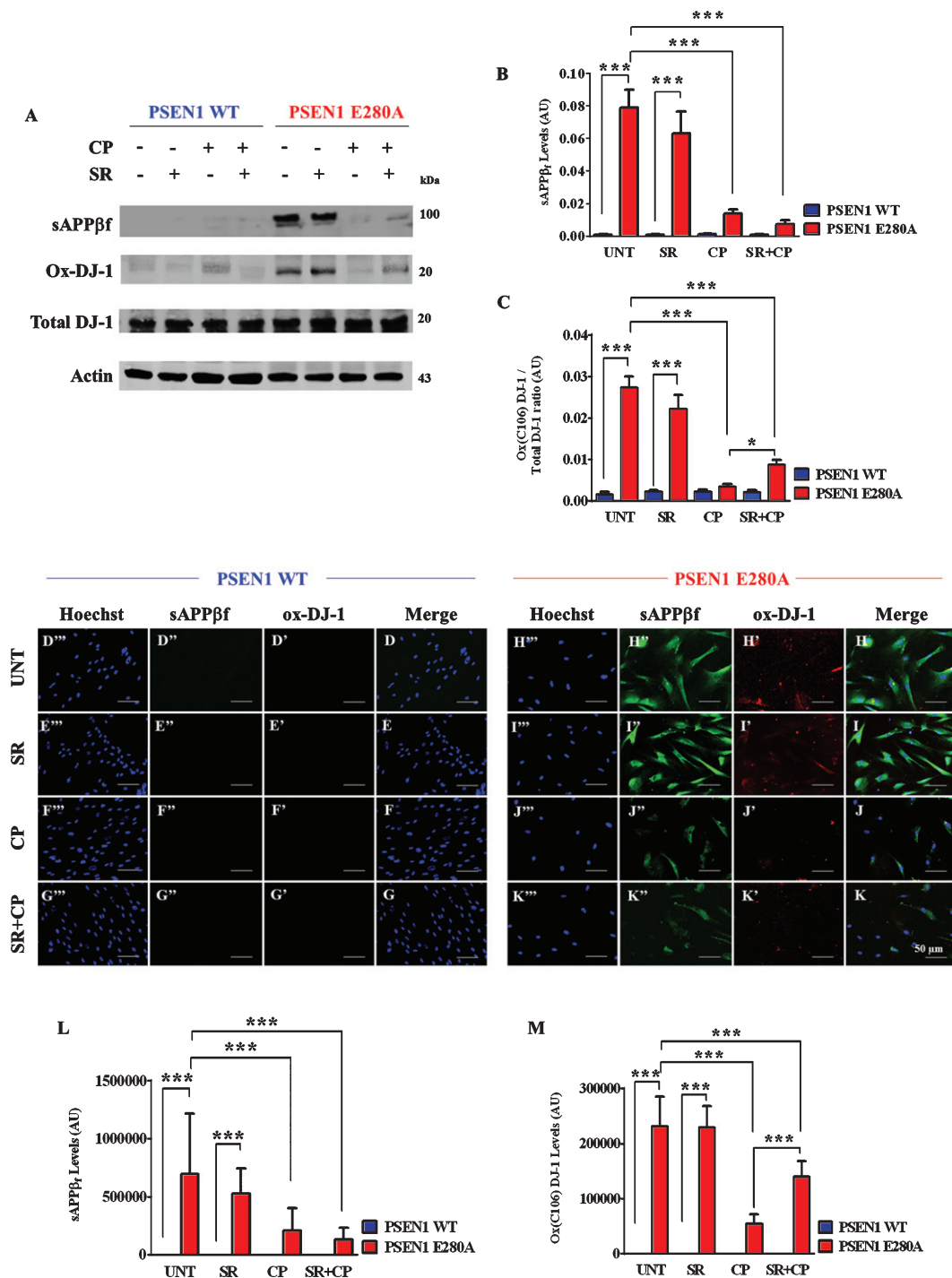
Fig. 3. CP55940 reduced intracellular sAβPPβf and oxidized DJ-1 independent of CB$_1$Rs in PSEN1 E280A ChLNs. After 7 days of transdifferentiation, WT PSEN1 and PSEN1 E280A ChLNs were left untreated or treated with SR, CP, or SR + CP in RCm for 4 days. Further, the proteins in the extracts were blotted with primary antibodies against Aβ$_{42}$, oxDJ-1Cys[106], and actin proteins. The intensities of the western blot bands shown in (A) were measured (B, C) by an infrared imaging system (Odyssey, LI-COR), and the intensity was normalized to that of actin. Additionally, cells were double-stained as indicated in the figure (D-K) with primary antibodies against oxDJ-1Cys[106] (*red*; D'-K') and APP$_{751}$/ Aβ$_{42}$ (*green*; D''- K''). The nuclei were stained with Hoechst 33342 (*blue*; D'''- K'''). L) Quantification of Aβ$_{42}$ fluorescence intensity. M) Quantification of oxDJ-1Cys[106] fluorescence intensity. Data are expressed as the mean ± SD; *p < 0.05; **p < 0.01; ***p < 0.001. The blots and figures represent 1 out of 3 independent experiments. Image magnification, 200×.
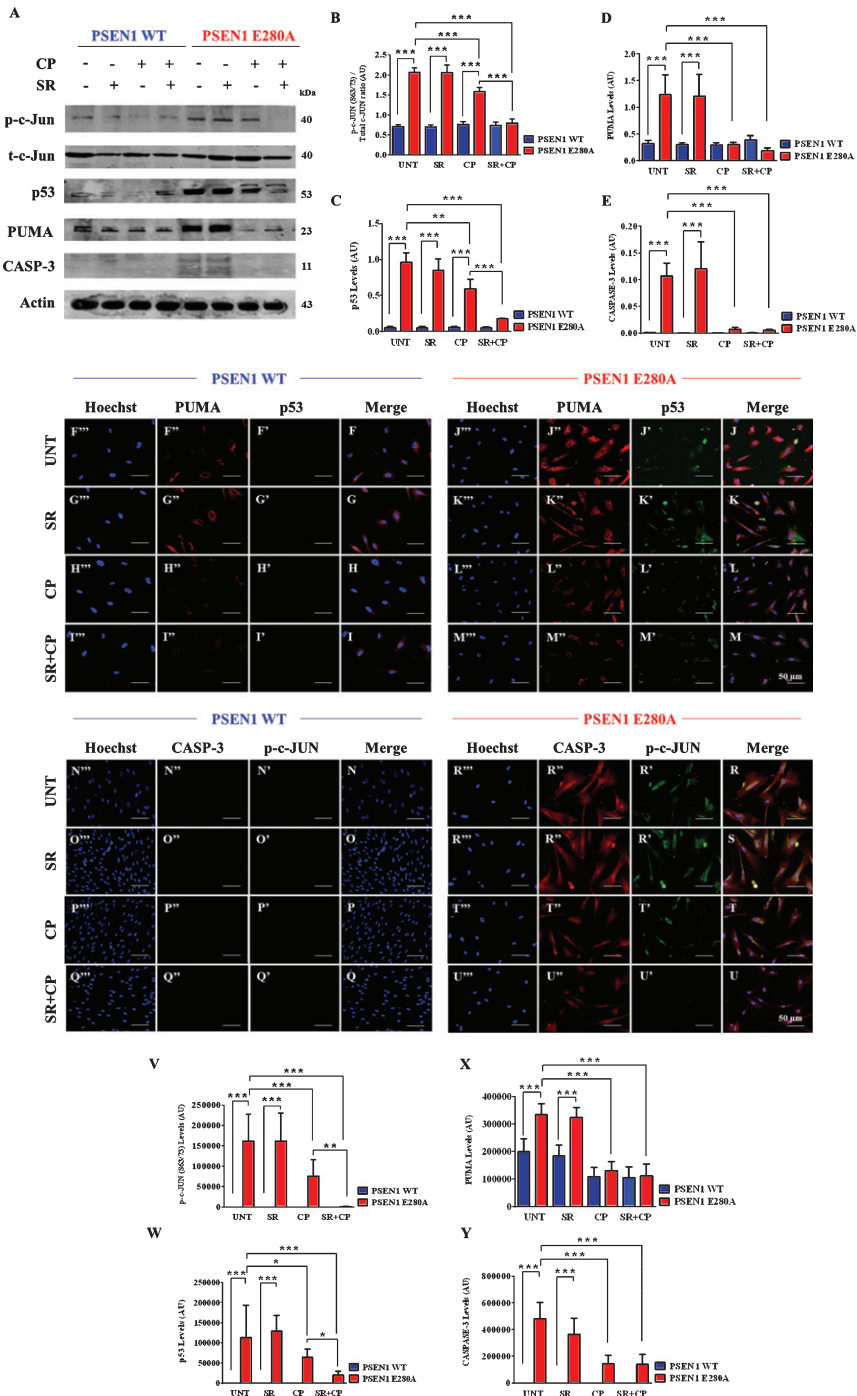
Fig. 4. CP55940 reduced the activation of p53, PUMA, c-Jun, and caspase-3 independent of CB$_1$Rs signaling in PSEN1 E280A ChLNs. After 7 days of transdifferentiation, WT PSEN1 and PSEN1 E280A ChLNs were left Untreated or treated with SR, CP, or SR + CP in regular culture medium for 4 days. After this time, the proteins in the extracts were blotted with primary antibodies against phosphorylated c-Jun (p-c-JUN)/total c-Jun, p53, PUMA, caspase-3 (CASP-3) and actin proteins. The intensities of the western blot bands shown in (A) were measured (B-E) by an infrared imaging system (Odyssey, LI-COR), and the intensity was normalized to that of actin. Additionally, cells were double-stained as indicated in the figure (F-U) with primary antibodies against p53 (*green*; F'-M'), PUMA (*red*; F"-M"), c-JUN (*green*; N'-U'), and CASP-3 (*red*; N"-U"). The nuclei were stained with Hoechst 33342 (*blue*; F"'-U"'). V-X) Quantification of c-JUN (V), p53 (W), PUMA (X), and CASP-3 (Y) fluorescence intensity. Data are expressed as the mean ± SD; *p < 0.05; **p < 0.01; ***p < 0.001. The blots and figures represent 1 out of 3 independent experiments. Image magnification, 200×.

CP + SR displayed almost basal levels of all proteins comparable to WT ChLNs. These observations were confirmed by fluorescent microscopy (Fig. 4F–Y).

CP55940 inhibits tau phosphorylation in a CB_1Rs-independent fashion PSEN1 E280A ChLNs

It has been established that intracellular sAβPPβf induce phosphorylation of tau [16]. We then investigated whether CP could inhibit tau phosphorylation in PSEN1 E280A ChLNs. As shown in Fig. 5, while the level of tau phosphorylation was detected to a similar extend in WT ChLNs under any experimental conditions (Fig. 5A, B), CP or CP + SR cocktail dramatically reduced phosphorylation of protein tau when compared to untreated or SR only treatment in mutant ChLNs (Fig. 5A, B). No statistically differences were observed between CP and CP + SR treatments in mutant ChLNs (Fig. 5B). These observations were confirmed by fluorescent microscopy (Fig. 5C–K).

CP55940 reduces the levels of eAβ42 protein fragment independent of CB_1Rs in PSEN 1 E280A ChLNs

Based on the observation that CP inhibited the intracellular aggregation of sAβPPβf (see Fig. 3), we assessed whether CP could have the same effect on eAβ42 [16]. Effectively, CP and CP + SR but not SR only significantly diminished the amounts of eAβ42 compared to untreated neurons in mutant ChLNs according to the ELISA technique (Fig. 6). No statistically differences were observed between CP and CP + SR treatments in mutant ChLNs (Fig. 6). The amount of eAβ42 was not affected by any of the treatments in WT ChLNs (Fig. 6).

CP55940 does not recover Ca^{2+} dysregulation in PSEN1 E280A ChLNs

The above observations prompted us to test whether CP could ameliorate the physiological response of mutant ChLNs to ACh neurotransmitter stimuli. As expected, ACh induced a transient elevation of intracellular Ca^{2+} in WT ChLNs (control, the average maximum fluorescence change ($\Delta F/F$) was 3.95 ± 0.19 at 10 s ($n = 20$ ChLN cells imaged, $N = 3$ dishes were used as a standard condition in this and following experiments) according to cytoplasmic Ca^{2+} responses to Fluo-3-mediated

imaging (Fig. 7A, E). We found no statistical differences between SR (Fig. 7B, E, $\Delta F/F = 5.05 \pm 0.35$), SR + CP (Fig. 7D, E; $\Delta F/F = 4.31 \pm 0.26$) and untreated conditions (Fig. 7E). In contrast, CP only and ACh significantly depressed intracellular Ca^{2+} (by –68%) in WT ChLNs (Fig. 7C, E, $\Delta F/F = 2.35 \pm 0.12$). When mutant neurons were exposed to ACh only (Fig. 7F, J, $\Delta F/F = 0.02 \pm 0.00$) and CP (Fig. 7H, J, $\Delta F/F = 0.06 \pm 0.00$), mutant cells were irresponsive to both stimuli (Fig. 7J). Interestingly, while SR only slightly increased intracellular Ca^{2+} (Fig. 7G, J, $\Delta F/F = 0.63 \pm 0.07$), the CP + SR cocktail and ACh increased inflow Ca^{2+} (Fig. 7H, J, $\Delta F/F = 3.32 \pm 0.23$) in PSEN 1 E280A ChLNs to similar extend as $[Ca^{2+}]i$ in WT ChLNs (Fig. 7E, J).

Anti-Aβ42 antibodies completely recuperate Ca^{2+} influx in PSEN1 E280A ChLNs

Since PSEN1 E280A ChLNs response to ACh decline in a time-dependent fashion [16], and since SR alone treatment was innocuous for WT and E280A ChLNs, we evaluated whether early inhibition of eAβ42 by anti-Aβ antibodies could ameliorate the mutant ChLNs response to ACh under CP and CP + SR treatments. As shown in Fig. 8, incubation of WT with anti-Aβ antibody 6E10 only (Fig. 8A, D; $\Delta F/F = 4.27 \pm 0.21$) or in the presence of CP (Fig. 8B, D; $\Delta F/F = 3.11 \pm 0.25$) or CP + SR (Fig. 8C, D; $\Delta F/F = 4.01 \pm 0.20$) showed similar transient intracellular Ca^{2+}. We found no statistical differences between those treatments (Fig. 8D). Remarkably, ACh and the anti-Aβ antibody 6E10 completely recovered Ca^{2+} influx in mutant ChLNs (Fig. 8E, H; $\Delta F/F = 3.37 \pm 0.20$). The anti-Aβ antibody 6E10 and CP (Fig. 8F, H; $\Delta F/F = 5.78 \pm 0.87$) and antibody + CP + SR (Fig. 8G, H; $\Delta F/F = 5.93 \pm 0.29$) dramatically induced a transient elevation of intracellular Ca^{2+} in mutant ChLNs (Fig. 8H).

DISCUSSION

In the present investigation, we demonstrate that CP inhibits the aggregation of (i)sAβPPβf, and p-Tau, increases $\Delta\Psi_m$, inhibits the generation of ROS and oxidation of DJ-1Cys106-SH to DJ-1Cys106-SO3, blocks the activation of the transcription factor p53 and c-Jun, pro-apoptotic protein PUMA, and protease caspase-3—all markers of cell death by apoptosis, and reduce eAβ42 in a CB_1R-dependent and-independent fashion in PSEN1 E280A ChLNs, used as a neuronal cell model of FAD [16]. Although
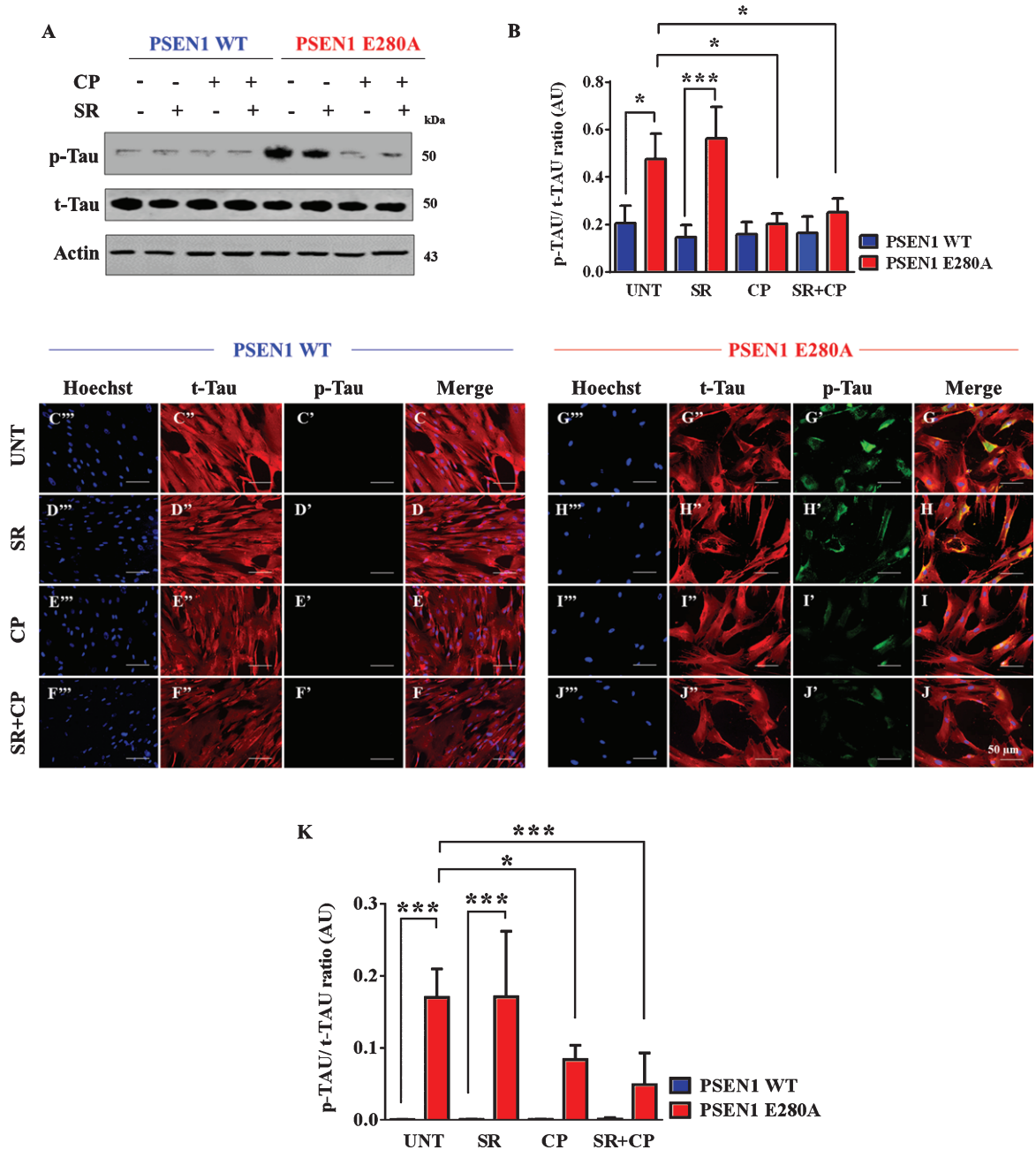
Fig. 5. CP55940 reduced the phosphorylation of tau protein independent of CB$_1$Rs in PSEN1 E280A ChLNs. After 7 days of transdifferentiation, WT PSEN1 and PSEN1 E280A ChLNs were left untreated or treated with SR, CP, or SR + CP in regular culture medium for 4 days. After this time, the proteins in the extracts were blotted with primary antibodies against phosphorylated tau (p-Tau), total tau (t-Tau), and actin proteins. The intensities of the western blot bands shown in (A) were measured (B) by an infrared imaging system (Odyssey, LI-COR), and the p-Tau/t-Tau ratio was normalized to that of actin. Additionally, cells were double-stained as indicated in the figure (C-J) with primary antibodies against p-Tau (*green*; C'-J') and t-Tau (*red*; C"-J"). The nuclei were stained with Hoechst 33342 (*blue*; C'''-J'''). K) Quantification of the p-Tau/t-Tau fluorescence ratio. Data are expressed as the mean ± SD; *p < 0.05; **p < 0.01; ***p < 0.001. The blots and figures represent 1 out of 3 independent experiments. Image magnification, 200×.

CP was unable to reverse the Ca^{2+} influx dysregulation as a response to ACh stimuli, it is demonstrated that CP affects several cellular molecular targets.

Several observations support these assumptions. First, in agreement with previous work [27], we found that CP reduced OS by directly scavenging ROS
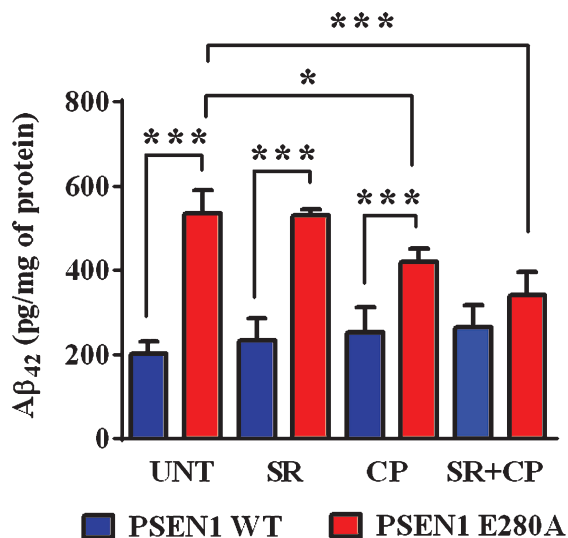
Fig. 6. CP55940 reduced the levels of extracellular $A\beta_{42}$ peptide in PSEN1 E280A ChLNs by a CB_1R-independent mechanism. After 7 days of transdifferentiation, WT PSEN1 and PSEN1 E280A ChLNs were left untreated or treated with SR, CP, or SR + CP in RCm for 4 days. ELISA quantification of extracellular $A\beta_{42}$ peptide in supernatants. Data are presented as means ± SD. *$p < 0.05$; **$p < 0.01$; ***$p < 0.001$. The histograms and figures represent 1 out of 4 independent experiments.

(e.g., H_2O_2) [22–28] and partially diminished ROS through CB_1Rs signaling. These observations may indicate that CP operates in a dual-way: as an antioxidant and as a CB_1Rs ligand. Second, CP dramatically increases the $\Delta\Psi_m$ in PSEN1 E280A ChLNs. Several data indicate that CP and other cannabinoids (e.g., THC, arachidonyl-2-chloroethylamide) can protect mitochondria against OS stimuli by inhibition of mitochondria permeability transition pore (mPTP) opening [37] or through activation of mitochondrial (mt)CB_1Rs [38, 39]. Even though, mtCB_1Rs activation have been linked to an intra-mitochondrial signaling cascade involving lessening of the activity of the electron transport system, oxygen consumption, and ATP production [40], our data favor the view that inhibition of mPTP opening by CP might be responsible for neuroprotective action on mutant ChLNs [37]. Indeed, it has been shown that the CB_2 agonist JWH-015 attenuated mitochondrial damage against OS stimuli by scavenging anion superoxide radical ($O_2^{\cdot-}$) and H_2O_2, maintaining $\Delta\Psi_m$ and avoiding Ca^{2+}-induced mitochondrial swelling [37]. Additionally, CP may indirectly protect mitochondria by blocking the interaction of $sA\beta PP\beta f$ and mitochondrial respiratory complexes [41, 42] or
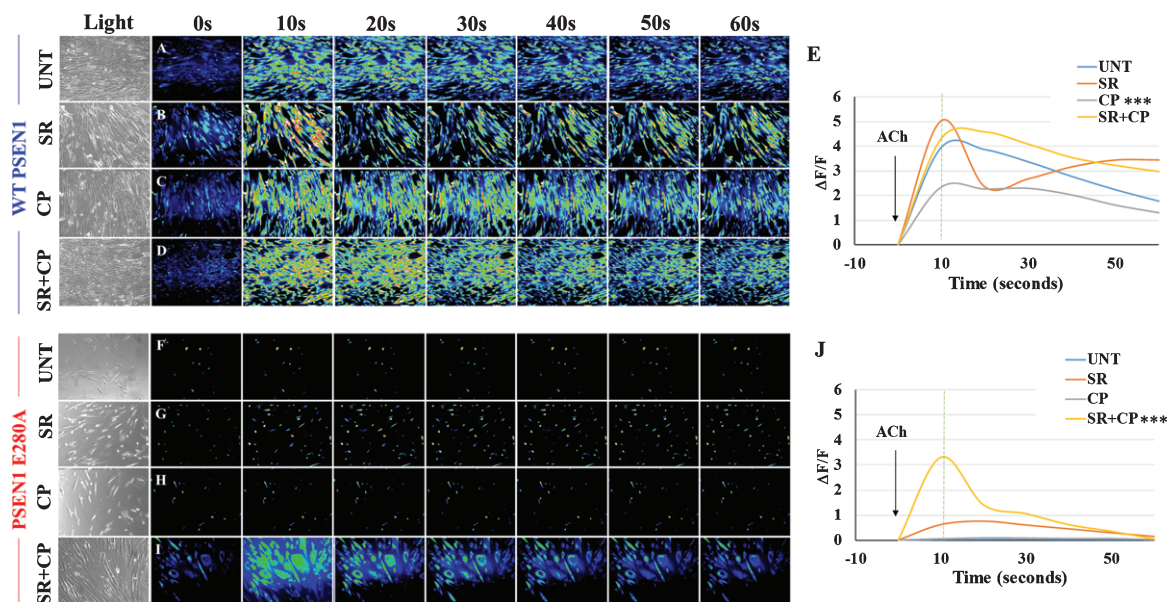

Fig. 7. CP55940 does not recover Ca^{2+} dysregulation in PSEN1 E280A ChLNs. After 7 days of transdifferentiation, WT PSEN1 and PSEN1 E280A ChLNs were left untreated or treated with SR, CP, or SR + CP in regular culture medium for 4 days. A-D, F-I) Time-lapse images (0, 10, 20, 30, 40, 50, and 60 s) of Ca^{2+} fluorescence in WT PSEN1 and PSEN1 E280A ChLNs on day 4 in response to ACh treatment. ACh was puffed into the culture at 0 s (*arrow*). Then, the Ca^{2+} fluorescence of the cells was monitored at the indicated times. Color contrast indicates fluorescence intensity: dark blue < light blue < green<yellow<red. E, J) Normalized mean fluorescence signal ($\Delta F/F$) over time from the cells indicating temporal cytoplasmic Ca^{2+} elevation in response to ACh treatment. Data are presented as the mean ± SD. *$p < 0.05$; **$p < 0.01$; ***$p < 0.001$ compared to UNT. The histograms and figures represent 1 out of 3 independent experiments. Image magnification, 200×.
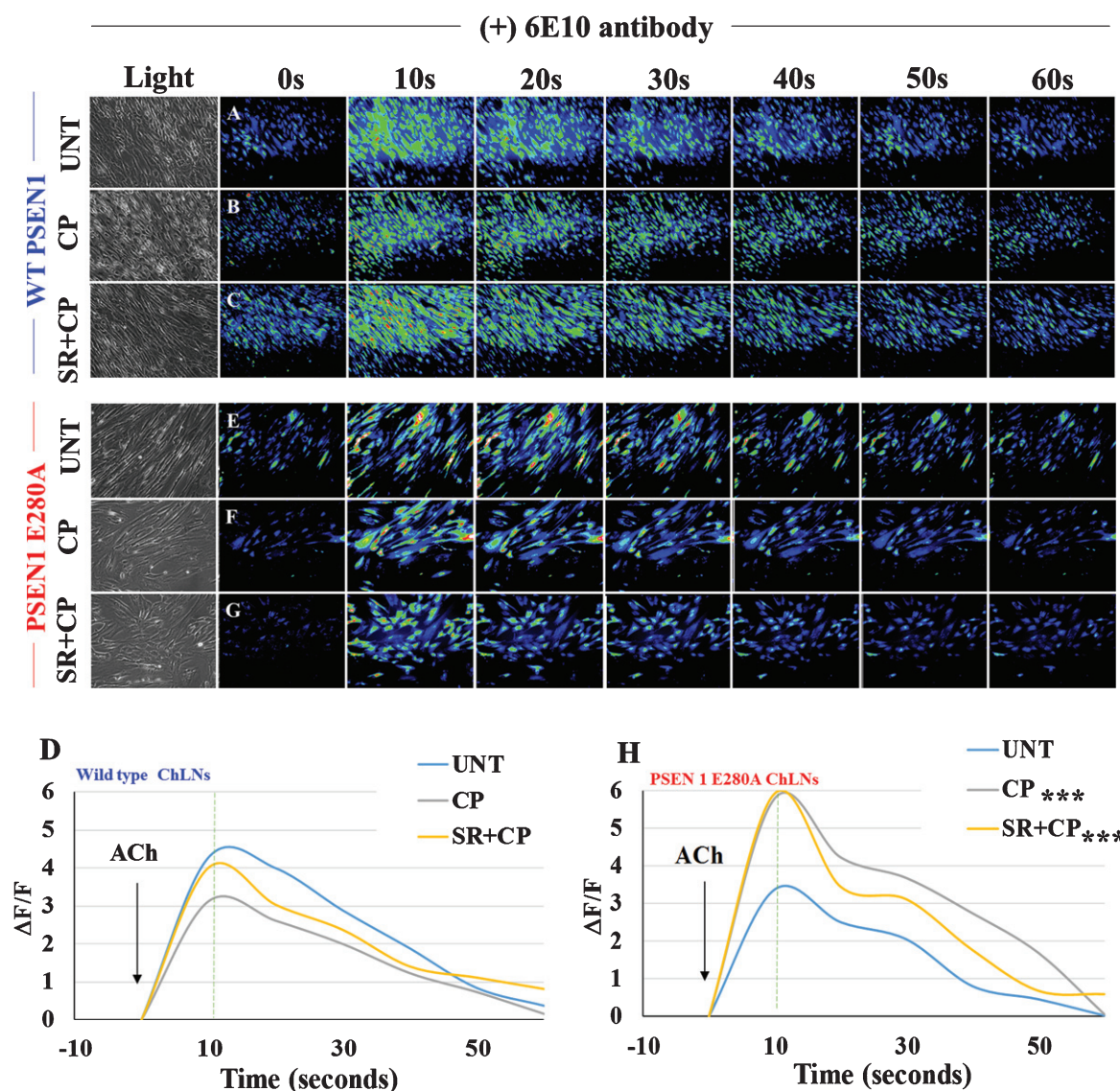
Fig. 8. CP55940 plus SR and anti-Aβ_{42} antibody 6E10 completely recover Ca^{2+} influx in PSEN1 E280A ChLNs. After 7 days of transdifferentiation, WT PSEN1 and PSEN1 E280A ChLNs were incubated with 6E10 antibody as described in Materials and Methods section. Simultaneously cells were left untreated or treated with CP or SR + CP in RCm for 4 days. A-C, E-G) Time-lapse images (0, 10, 20, 30, 40, 50, and 60 s) of Ca^{2+} fluorescence in WT PSEN1 and PSEN1 E280A ChLNs at day4 in the presence of 6E10 antibody as a response to ACh treatment. ACh was puffed into the culture at 0 s (arrow). Then, the Ca^{2+} fluorescence of the cells was monitored at the indicated times. Color contrast indicates fluorescence intensity: dark blue < light blue < green<yellow<red. D, H) Normalized mean fluorescence signal (ΔF/F) over time from the cells indicating temporal cytoplasmic Ca^{2+} elevation in response to ACh treatment. Data are presented as means ± SD. *p < 0.05; **p < 0.01; ***p < 0.001 compared to UNT. The histograms and figures represent 1 out of 3 independent experiments. Image magnification, 200×.

by inhibition of mitochondria-targeted pro-apoptotic proteins (e.g., PUMA, this work). Taken together our findings suggest that CP reverses the loss of $\Delta\Psi_m$ and mitochondria damage independently of plasma membrane CB$_1$ receptors or (mt)CB$_1$Rs. Third, it is known that cannabinoids (e.g., THC) stimulate the removal of intracellular Aβ through a dependent [43] or

independent CB$_1$Rs mechanism [22]. Here, we report for the first time that CP inhibits the aggregation of (i)sAβPPβf in PSEN1 E280A ChLNs independently of CB$_1$ receptor signaling. Since Aβ_{42} is still detected extracellularly in mutant neurons treated with CP, it might imply that this cannabinoid does not interfere with the AβPP metabolism. Finally, CP significantly

diminished oxidation of protein DJ-1, as evidence of OS. Because DJ-1Cys[106]SH residue is specifically sensible to H_2O_2 oxidation [44], it is likely that CP might directly interact with ROS or induces its suppression via CB_1Rs activation. Taken together our results comply with the view that early aggregation of (i)sAβPPβf and generation of H_2O_2 can be blocked by the direct action of cannabinoid CP and by partial activation of CB_1Rs, respectively.

Recent data have shown that (i)sAβPPβf (/H_2O_2) induce activation of JNK/c-Jun and p53, which in turn activate PUMA and caspase-3 [16]. Interestingly, we found that CP blocks activation of transcription factors c-Jun, p53, PUMA, and caspase-3 independently of CB_1Rs stimulation. These observations suggest that CP exerted a direct role in protecting PSEN1 E280A ChLNs against endogenously OS-induced cell death signaling. Since downregulation of c-Jun and p53 may reduce transcription of PUMA [45–47], CP may restrain mitochondria from leaking pro-apoptogenic proteins such as caspase-9, and ensuing activation of caspase-3. These actions avoid neuronal dismantling and increase the survival of mutant ChLNs.

Previously, it has been shown that (i)sAβPPβf induces p-Tau through JNK kinase in PSEN 1 E280A ChLNs [16]. In this work, we demonstrate that CP almost completely inhibits the phosphorylation of protein tau independently of CB_1Rs. One possible explanation is that CP can suppress H_2O_2 generation, which serves as a messenger molecule that triggers activation of JNK [48, 49], and phosphorylation of tau [50]. It is therefore not surprising that p-Tau was untraceable in PSEN1 E280A ChLNs. However, we do not discard the possibility that CP blocks p-Tau by alternative CB_1Rs-independent mechanisms in ChLNs [51].

Mounting evidence has demonstrated that eAβ is neurotoxic before the appearance of plaques [16, 52, 53]. Interestingly, CP reduced the amounts of eAβ$_{42}$ in a CB_1Rs-independent manner. This observation suggests that CP directly modulates intracellular and extracellular AβPP-derived protein fragments. However, the action of CP on eAβ$_{42}$ did not impact on the response of mutant ChLNs to ACh stimuli. Here, we confirm that ACh receptors (AChRs) are physiologically altered in PSEN 1 E280A ChLNs [16] most probably through Aβ-induced inhibition of nicotinic (n)AChRs [54, 55], which normally revealed a rapid elevation of intracellular Ca^{2+} [56–58] as shown in WT ChLNs. Indeed, AChRs were irresponsive to ACh stimuli, thereby nullifying the transient rise

of intracellular Ca^{2+} in mutant ChLNs (i.e., –99% reduction in $[Ca^{2+}]_i$) compared to wild type ChLNs. On the other hand, CP decreased $[Ca^{2+}]_i$ by –68% in WT ChLNs. These observations suggest that CP either directly inhibited the function of AChRs [59, 60] and/ or inhibited the inflow of Ca^{2+} via activation of CB_1Rs on calcium channels (e.g., T, N- and P/Q-type [20]). Since the response of PSEN 1 E280A ChLNs to ACh is already compromised, CP was not able to modify the influx of Ca^{2+} when challenged with the neurotransmitter. Interestingly, SR only or with CP increased $[Ca^{2+}]_i$ in PSEN 1 E280A ChLNs compared to untreated mutant ChLNs. This positive improvement of Ca^{2+} inflow was comparable to WT ChLNs (see CP + SR effect on neurons). These observations can be explained by the fact that SR can either stimulate Ca^{2+} influx through Ca^{2+} channels (e.g., Ca_v2: N-, P/Q channels [61]) or block the negative interaction of CP with nAChRs in WT ChLNs when exposed to ACh (this work). Our findings suggest that CB_1Rs are marginally active in PSEN 1 E280A ChLNs. Interestingly; anti-Aβ$_{42}$ antibody completely recovered transient intracellular Ca^{2+} signal in mutant ChLNs. The Ca^{2+} signal was further increased when neurons were co-cultured with CP only or SR plus CP. These last observations reinforce the view that Aβ$_{42}$ and SR interfere with CP and AChRs. Similar to PSEN 1 E280A ChLNs, antibody anti-Aβ$_{42}$ increased transient intracellular Ca^{2+} signals in WT ChLNs. These observations imply that eAβ$_{42}$ secreted in low amounts by WT ChLNs or abnormally secreted in high amounts by mutant ChLNs is an AChRs regulator in ChLNs. Taken together these observations suggest that a combination of CP with anti-Aβ$_{42}$ would be therapeutically beneficial to FAD patients.

Conclusion

In an attempt to modify the neuropathological expression of ChLNs bearing the mutation PSEN1 E280A (e.g., intracellular aggregation of sAβPPβf, tau phosphorylation, OS, apoptosis, and Ca^{2+} influx dysfunction) (Fig. 9A), we found that cannabinoid CP is a multi-target molecule that promotes the recovery FAD cholinergic neurons by increasing $\Delta\Psi_m$, impedes phosphorylation of protein tau, and blocks OS-induced apoptosis signaling (Fig. 9B). However, CP was unable to modify the neuronal functionality as evidenced by an inability of ACh to increase Ca^{2+} influx in PSEN1 E280A ChLNs. Since the nature of

the neuronal cholinergic dysfunctionality stems from the blocking of nAChRs by $A\beta_{42}$ [54, 55], drugs that interfere with the interaction of $A\beta$ and the AChRs might ameliorate the ligand-gated ion Ca^{2+} channel interactions (e.g., [62]). In this respect, we show that anti-$A\beta_{42}$ antibody 6E10 plus CP or anti-$A\beta_{42}$ and SR + CP change mutant ChLNs response to ACh by increasing Ca^{2+} influx to similar $[Ca^{2+}]_i$ in WT ChLNs (Fig. 9C, D). It is therefore proposed that combinations of cannabinoids, anti-$A\beta_{42}$ antibodies (e.g., crenezumab [63, 64]), and CB_1 inverse agonists might be a promising multi-target drugs for therapy [65] in the early treatment of FAD PSEN 1 E280A ChLNs neurodegeneration.
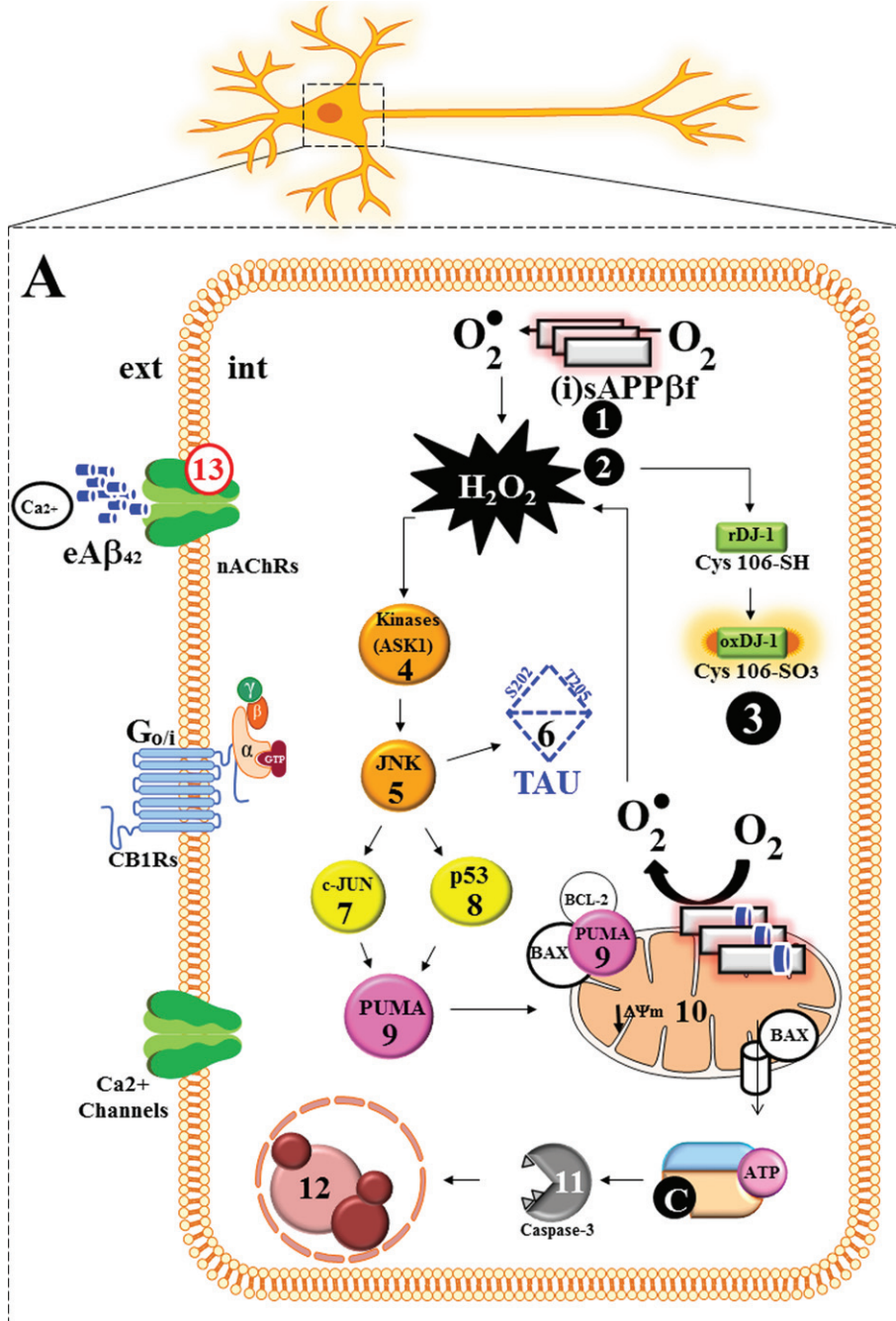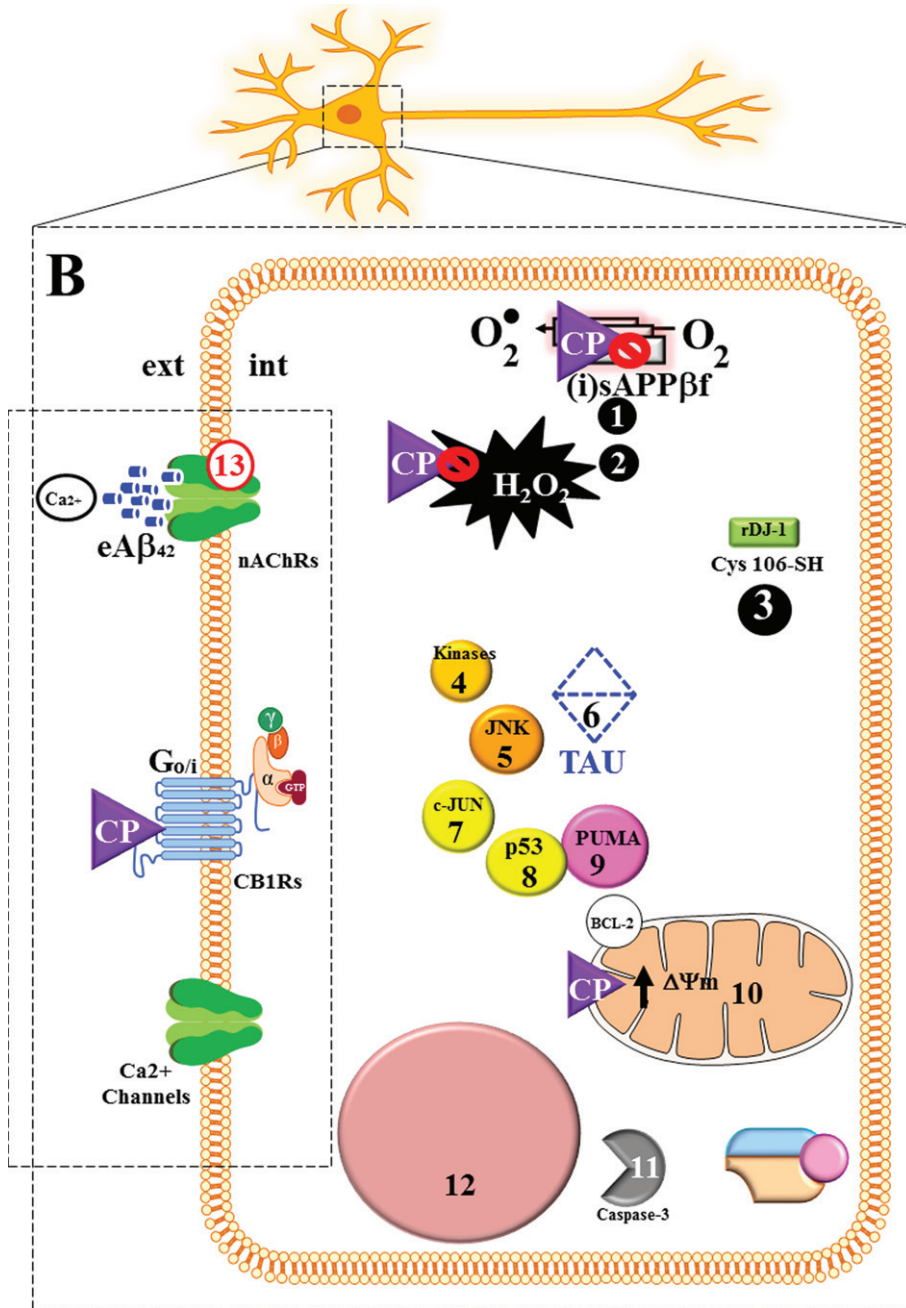

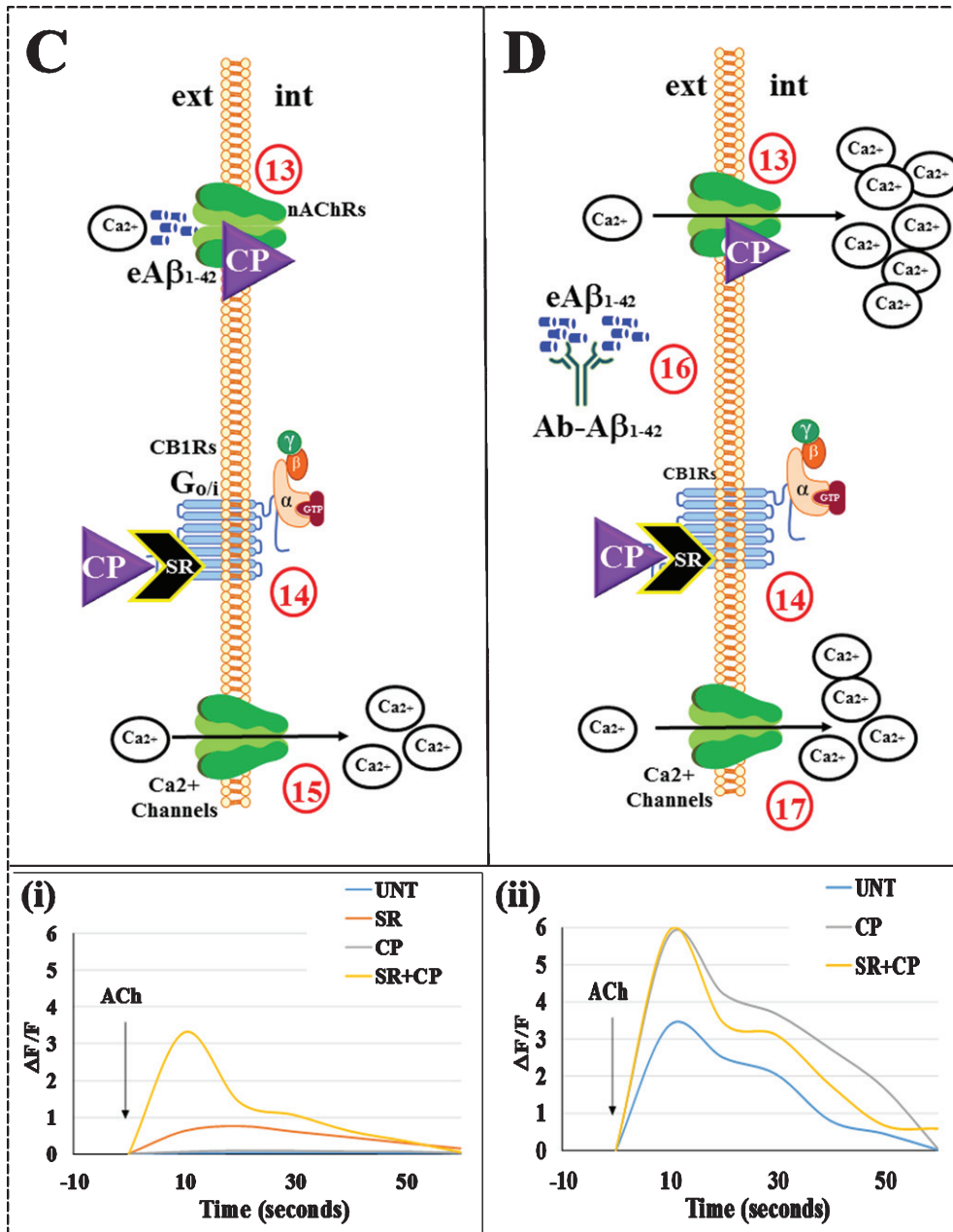Fig. 9. (*Continued*)

Fig. 9. (*Continued*)

Fig. 9. Schematic representation of the protective effect of CP55940 on PSEN 1 E280A ChLNs. A) Intracellularly accumulation of sAβPPβf (step 1) generates H_2O_2 (s2), which in turn oxidized the OS sensor protein DJ-1 at Cys-[106]-SH residue into DJ-1Cys[106]-SO_3 (s3) and activates a domino-like pro-death signaling mechanism by triggering kinases (s4, e.g., ASK1) and JNK kinase (s5). This last kinase phosphorylates protein tau (s6) and activates the transcription factors c-Jun (s7) and p53 (s8). Both transcription factors transcribe the BH-3-only protein PUMA (s9), which together with other pro-apoptosis proteins (e.g., BAX), it induces depolarization of mitochondria, opening of the mitochondrial transition pore, and loss of mitochondrial membrane potential ($\Delta\Psi_m$, s10). Damage of mitochondria potential provokes the release of pro-apoptogenic protein cytochrome C, ensuing activation of caspase-3 (s11). In turn, this protease activates the endonuclease DFF40 by cleaving the nuclease's inhibitor DFF45. Finally, DFF40 causes the nuclear chromatin fragmentation, typical of apoptosis (s12). Additionally, ChLNs do not respond to ACh stimuli, i.e., intracellular transient Ca^{2+} increase is missing due to extracellular interaction between $A\beta_{42}$ ($eA\beta_{42}$) and nicotinic (n)ACh receptors (s13). The sAβPPβf-induced process (s1-s13) leads ChL neurons to structural alterations (e.g., aggregation/ hyperphosphorylation of protein tau), cell death (apoptosis) and intracellular Ca^{2+} dysfunction. B) Upon exposure to CP55940 (CP), ChLNs show normal features such as no oxidized protein DJ-1 (s3), unaltered $\Delta\Psi_m$ (s10), and intact nuclei

morphology (s12). Moreover, CP inhibits aggregation of sAβPPβf (s1), and blocks generation of H_2O_2 (s2) most probably by quenching anion superoxide radicals ($O_2^{·-}$). As a consequence, no further activation of kinases (s4, s5), phosphorylation of protein tau (s6), and c-Jun (s7), and activation of p53 (s8), PUMA (s9), and caspase-3 (s11) occurs in PSEN1 E280A ChLNs just leaving mitochondria and nuclei unchanged from sAβPPβf-induced damage. C) Since nAChRs are blocked by eAβ$_{42}$ (s13), CP was unable to modify the response of mutant ChLNs to ACh (inset graph i). Interestingly, the CB_1 and CB_2 receptor inverse agonists SR141716 plus SR144528 (= SR) only or in the presence of CP induce a significant increase in intracellular Ca^{2+} (s14) most probably through activation of Ca^{2+} channels (s15 and inset graph i). D) When mutant ChLNs were exposed to CP, SR, and anti-Aβ$_{42}$ antibody 6E10 (s16), the mixture induced a dramatic increase in the transient intracellular Ca^{2+} flow (s13, s17 and inset graph ii).

ACKNOWLEDGMENTS

REFERENCES

[1] Long JM, Holtzman DM (2019) Alzheimer disease: An update on pathobiology and treatment strategies. *Cell* **179**, 312-339.

[2] Hampel H, Mesulam MM, Cuello AC, Farlow MR, Giacobini E, Grossberg GT, Khachaturian AS, Vergallo A, Cavedo E, Snyder PJ, Khachaturian ZS (2018) The cholinergic system in the pathophysiology and treatment of Alzheimer's disease. *Brain* **141**, 1917-1933.

[3] DeTure MA, Dickson DW (2019) The neuropathological diagnosis of Alzheimer's disease. *Mol Neurodegener* **14**, 32.

[4] Yuksel M, Tacal O (2019) Trafficking and proteolytic processing of amyloid precursor protein and secretases in Alzheimer's disease development: An up-to-date review. *Eur J Pharmacol* **856**, 172415.

[5] Kabir MT, Uddin MS, Setu JR, Ashraf GM, Bin-Jumah MN, Abdel-Daim MM (2020) Exploring the role of PSEN mutations in the pathogenesis of Alzheimer's disease. *Neurotox Res* **38**, 833-849.

[6] Sun L, Zhou R, Yang G, Shi Y (2017) Analysis of 138 pathogenic mutations in presenilin-1 on the *in vitro* production of Abeta42 and Abeta40 peptides by gamma-secretase. *Proc Natl Acad Sci U S A* **114**, E476-E485.

[7] Lopera F, Ardilla A, Martinez A, Madrigal L, Arango-Viana JC, Lemere CA, Arango-Lasprilla JC, Hincapie L, Arcos-Burgos M, Ossa JE, Behrens IM, Norton J, Lendon C, Goate AM, Ruiz-Linares A, Rosselli M, Kosik KS (1997) Clinical features of early-onset Alzheimer disease in a large kindred with an E280A presenilin-1 mutation. *JAMA* **277**, 793-799.

[8] Sepulveda-Falla D, Glatzel M, Lopera F (2012) Phenotypic profile of early-onset familial Alzheimer's disease caused by presenilin-1 E280A mutation. *J Alzheimers Dis* **32**, 1-12.

[9] Fuller JT, Cronin-Golomb A, Gatchel JR, Norton DJ, Guzman-Velez E, Jacobs HIL, Hanseeuw B, Pardilla-Delgado E, Artola A, Baena A, Bocanegra Y, Kosik KS, Chen K, Tariot PN, Johnson K, Sperling RA, Reiman EM, Lopera F, Quiroz YT (2019) Biological and cognitive markers of presenilin1 E280A autosomal dominant Alzheimer's disease: A comprehensive review of the Colombian kindred. *J Prev Alzheimers Dis* **6**, 112-120.

[10] Lalli MA, Cox HC, Arcila ML, Cadavid L, Moreno S, Garcia G, Madrigal L, Reiman EM, Arcos-Burgos M, Bedoya G, Brunkow ME, Glusman G, Roach JC, Hood L, Kosik KS, Lopera F (2014) Origin of the PSEN1 E280A mutation causing early-onset Alzheimer's disease. *Alzheimers Dement* **10**, S277-S283.e210.

[11] Zhou R, Yang G, Shi Y (2017) Dominant negative effect of the loss-of-function gamma-secretase mutants on the wild-type enzyme through heterooligomerization. *Proc Natl Acad Sci U S A* **114**, 12731-12736.

[12] Lemere CA, Lopera F, Kosik KS, Lendon CL, Ossa J, Saido TC, Yamaguchi H, Ruiz A, Martinez A, Madrigal L, Hincapie L, Arango JC, Anthony DC, Koo EH, Goate AM, Selkoe DJ (1996) The E280A presenilin 1 Alzheimer mutation produces increased A beta 42 deposition and severe cerebellar pathology. *Nat Med* **2**, 1146-1150.

[13] Velez-Pardo C, Arellano JI, Cardona-Gomez P, Jimenez Del Rio M, Lopera F, De Felipe J (2004) CA1 hippocampal neuronal loss in familial Alzheimer's disease presenilin-1 E280A mutation is related to epilepsy. *Epilepsia* **45**, 751-756.

[14] Fleisher AS, Chen K, Quiroz YT, Jakimovich LJ, Gomez MG, Langois CM, Langbaum JB, Ayutyanont N, Roontiva A, Thiyyagura P, Lee W, Mo H, Lopez L, Moreno S, Acosta-Baena N, Giraldo M, Garcia G, Reiman RA, Huentelman MJ, Kosik KS, Tariot PN, Lopera F, Reiman EM (2012) Florbetapir PET analysis of amyloid-β deposition in the presenilin 1 E280A autosomal dominant Alzheimer's disease kindred: A cross-sectional study. *Lancet Neurol* **11**, 1057-1065.

[15] Quiroz YT, Sperling RA, Norton DJ, Baena A, Arboleda-Velasquez JF, Cosio D, Schultz A, Lapoint M, Guzman-Velez E, Miller JB, Kim LA, Chen K, Tariot PN, Lopera F, Reiman EM, Johnson KA (2018) Association between amyloid and tau accumulation in young adults with autosomal dominant Alzheimer disease. *JAMA Neurol* **75**, 548-556.

[16] Soto-Mercado V, Mendivil-Perez M, Velez-Pardo C, Lopera F, Jimenez-Del-Rio M (2020) Cholinergic-like neurons carrying PSEN1 E280A mutation from familial Alzheimer's disease reveal intraneuronal sAPPβ fragments accumulation, hyperphosphorylation of tau, oxidative stress, apoptosis and Ca2+dysregulation: Therapeutic implications. *PLoS One* **15**, e0221669.

[17] Bonini SA, Premoli M, Tambaro S, Kumar A, Maccarinelli G, Memo M, Mastinu A (2018) Cannabis sativa: A comprehensive ethnopharmacological review of a medicinal plant with a long history. *J Ethnopharmacol* **227**, 300-315.

[18] Cassano T, Villani R, Pace L, Carbone A, Bukke VN, Orkisz S, Avolio C, Serviddio G (2020) From Cannabis sativa to cannabidiol: Promising therapeutic candidate for the

treatment of neurodegenerative diseases. *Front Pharmacol* **11**, 124.

[19] ElSohly MA, Radwan MM, Gul W, Chandra S, Galal A (2017) Phytochemistry of Cannabis sativa L. *Prog Chem Org Nat Prod* **103**, 1-36.

[20] Marcu J, Schechter J (2016) Molecular pharmacology of CB1 and CB2 cannabinoid receptors. In *Neuropathology of Drug Addictions and Substance Misuse*, Preedy V, ed. Academic Press, pp. 713-721.

[21] Shahbazi F, Grandi V, Banerjee A, Trant JF (2020) Cannabinoids and cannabinoid receptors: The story so far. *iScience* **23**, 101301.

[22] Schubert D, Kepchia D, Liang Z, Dargusch R, Goldberg J, Maher P (2019) Efficacy of cannabinoids in a pre-clinical drug-screening platform for Alzheimer's disease. *Mol Neurobiol* **56**, 7719-7730.

[23] Hampson AJ, Grimaldi M, Axelrod J, Wink D (1998) Cannabidiol and (-)Delta9-tetrahydrocannabinol are neuroprotective antioxidants. *Proc Natl Acad Sci U S A* **95**, 8268-8273.

[24] Chen Y, Buck J (2000) Cannabinoids protect cells from oxidative cell death: A receptor-independent mechanism. *J Pharmacol Exp Ther* **293**, 807-812.

[25] Marsicano G, Moosmann B, Hermann H, Lutz B, Behl C (2002) Neuroprotective properties of cannabinoids against oxidative stress: Role of the cannabinoid receptor CB1. *J Neurochem* **80**, 448-456.

[26] Jimenez-Del-Rio M, Daza-Restrepo A, Velez-Pardo C (2008) The cannabinoid CP55,940 prolongs survival and improves locomotor activity in Drosophila melanogaster against paraquat: Implications in Parkinson's disease. *Neurosci Res* **61**, 404-411.

[27] Velez-Pardo C, Del Rio MJ (2006) Avoidance of Abeta[(25-35)] / (H(2)O(2))-induced apoptosis in lymphocytes by the cannabinoid agonists CP55,940 and JWH-015 via receptor-independent and PI3K-dependent mechanisms: Role of NF-kappaB and p53. *Med Chem* **2**, 471-479.

[28] Harvey BS, Ohlsson KS, Mååg JL, Musgrave IF, Smid SD (2012) Contrasting protective effects of cannabinoids against oxidative stress and amyloid-β evoked neurotoxicity *in vitro*. *Neurotoxicology* **33**, 138-146.

[29] Pertwee R, Cannabinoid Receptor Ligands, https://www.tocris.com/literature/scientific-reviews/cannabinoid-receptor-ligands, Accessed Aug. 2020.

[30] Mendivil-Perez M, Velez-Pardo C, Jimenez-Del-Rio M (2019) Direct transdifferentiation of human Wharton's jelly mesenchymal stromal cells into cholinergic-like neurons. *J Neurosci Methods* **312**, 126-138.

[31] Gulisano W, Melone M, Ripoli C, Tropea MR, Li Puma DD, Giunta S, Cocco S, Marcotulli D, Origlia N, Palmeri A, Arancio O, Conti F, Grassi C, Puzzo D (2019) Neuromodulatory action of picomolar extracellular Aβ42 oligomers on presynaptic and postsynaptic mechanisms underlying synaptic function and memory. *J Neurosci* **39**, 5986-6000.

[32] Armijo E, Gonzalez C, Shahnawaz M, Flores A, Davis B, Soto C (2017) Increased susceptibility to Abeta toxicity in neuronal cultures derived from familial Alzheimer's disease (PSEN1-A246E) induced pluripotent stem cells. *Neurosci Lett* **639**, 74-81.

[33] Pap P, Koszeghy A, Szucs G, Rusznak Z (2009) Cytoplasmic Ca(2+) concentration changes evoked by cholinergic stimulation in primary astrocyte cultures prepared from the rat cochlear nucleus. *Hear Res* **255**, 73-83.

[34] Sekiguchi-Tonosaki M, Obata M, Haruki A, Himi T, Kosaka J (2009) Acetylcholine induces Ca2+signaling in chicken retinal pigmented epithelial cells during dedifferentiation. *Am J Physiol Cell Physiol* **296**, C1195-1206.

[35] Lazic SE, Clarke-Williams CJ, Munafo MR (2018) What exactly is 'N' in cell culture and animal experiments? *PLoS Biol* **16**, e2005282.

[36] Nyíri G, Szabadits E, Cserép C, Mackie K, Shigemoto R, Freund TF (2005) GABAB and CB1 cannabinoid receptor expression identifies two types of septal cholinergic neurons. *Eur J Neurosci* **21**, 3034-3042.

[37] Velez-Pardo C, Jimenez-Del-Rio M, Lores-Arnaiz S, Bustamante J (2010) Protective effects of the synthetic cannabinoids CP55,940 and JWH-015 on rat brain mitochondria upon paraquat exposure. *Neurochem Res* **35**, 1323-1332.

[38] Benard G, Massa F, Puente N, Lourenco J, Bellocchio L, Soria-Gomez E, Matias I, Delamarre A, Metna-Laurent M, Cannich A, Hebert-Chatelain E, Mulle C, Ortega-Gutierrez S, Martin-Fontecha M, Klugmann M, Guggenhuber S, Lutz B, Gertsch J, Chaouloff F, Lopez-Rodriguez ML, Grandes P, Rossignol R, Marsicano G (2012) Mitochondrial CB(1) receptors regulate neuronal energy metabolism. *Nat Neurosci* **15**, 558-564.

[39] Ma L, Niu W, Yang S, Tian J, Luan H, Cao M, Xi W, Tu W, Jia J, Lv J (2018) Inhibition of mitochondrial permeability transition pore opening contributes to cannabinoid type 1 receptor agonist ACEA-induced neuroprotection. *Neuropharmacology* **135**, 211-222.

[40] Melser S, Pagano Zottola AC, Serrat R, Puente N, Grandes P, Marsicano G, Hebert-Chatelain E (2017) Functional analysis of mitochondrial CB1 cannabinoid receptors (mtCB1) in the brain. *Methods Enzymol* **593**, 143-174.

[41] Devi L, Prabhu BM, Galati DF, Avadhani NG, Anandatheerthavarada HK (2006) Accumulation of amyloid precursor protein in the mitochondrial import channels of human Alzheimer's disease brain is associated with mitochondrial dysfunction. *J Neurosci* **26**, 9057-9068.

[42] Anandatheerthavarada HK, Biswas G, Robin MA, Avadhani NG (2003) Mitochondrial targeting and a novel transmembrane arrest of Alzheimer's amyloid precursor protein impairs mitochondrial function in neuronal cells. *J Cell Biol* **161**, 41-54.

[43] Currais A, Quehenberger O, M Armando A, Daugherty D, Maher P, Schubert D (2016) Amyloid proteotoxicity initiates an inflammatory response blocked by cannabinoids. *NPJ Aging Mech Dis* **2**, 16012.

[44] Kinumi T, Kimata J, Taira T, Ariga H, Niki E (2004) Cysteine-106 of DJ-1 is the most sensitive cysteine residue to hydrogen peroxide-mediated oxidation *in vivo* in human umbilical vein endothelial cells. *Biochem Biophys Res Commun* **317**, 722-728.

[45] Nakano K, Vousden KH (2001) PUMA, a novel proapoptotic gene, is induced by p53. *Mol Cell* **7**, 683-694.

[46] Yu J, Zhang L, Hwang PM, Kinzler KW, Vogelstein B (2001) PUMA induces the rapid apoptosis of colorectal cancer cells. *Mol Cell* **7**, 673-682.

[47] Lu H, Hou G, Zhang Y, Dai Y, Zhao H (2014) c-Jun transactivates Puma gene expression to promote osteoarthritis. *Mol Med Rep* **9**, 1606-1612.

[48] Saitoh M, Nishitoh H, Fujii M, Takeda K, Tobiume K, Sawada Y, Kawabata M, Miyazono K, Ichijo H (1998) Mammalian thioredoxin is a direct inhibitor of apoptosis signal-regulating kinase (ASK) 1. *EMBO J* **17**, 2596-2606.

[49] Nishitoh H, Saitoh M, Mochida Y, Takeda K, Nakano H, Rothe M, Miyazono K, Ichijo H (1998) ASK1 is essential for JNK/SAPK activation by TRAF2. *Mol Cell* **2**, 389-395.

[50] Yoshida H, Hastie CJ, McLauchlan H, Cohen P, Goedert M (2004) Phosphorylation of microtubule-associated protein tau by isoforms of c-Jun N-terminal kinase (JNK). *J Neurochem* **90**, 352-358.

[51] Esposito G, De Filippis D, Carnuccio R, Izzo AA, Iuvone T (2006) The marijuana component cannabidiol inhibits beta-amyloid-induced tau protein hyperphosphorylation through Wnt/beta-catenin pathway rescue in PC12 cells. *J Mol Med (Berl)* **84**, 253-258.

[52] Lei M, Xu H, Li Z, Wang Z, O'Malley TT, Zhang D, Walsh DM, Xu P, Selkoe DJ, Li S (2016) Soluble Aβ oligomers impair hippocampal LTP by disrupting glutamatergic/GABAergic balance. *Neurobiol Dis* **85**, 111-121.

[53] Cline EN, Bicca MA, Viola KL, Klein WL (2018) The amyloid-beta oligomer hypothesis: Beginning of the third decade. *J Alzheimers Dis* **64**, S567-S610.

[54] Liu Q, Kawai H, Berg DK (2001) beta-Amyloid peptide blocks the response of alpha 7-containing nicotinic receptors on hippocampal neurons. *Proc Natl Acad Sci U S A* **98**, 4734-4739.

[55] Pettit DL, Shao Z, Yakel JL (2001) beta-Amyloid(1-42) peptide directly modulates nicotinic receptors in the rat hippocampal slice. *J Neurosci* **21**, RC120.

[56] Szabo GG, Lenkey N, Holderith N, Andrasi T, Nusser Z, Hajos N (2014) Presynaptic calcium channel inhibition underlies CB(1) cannabinoid receptor-mediated suppression of GABA release. *J Neurosci* **34**, 7958-7963.

[57] Shen JX, Yakel JL (2009) Nicotinic acetylcholine receptor-mediated calcium signaling in the nervous system. *Acta Pharmacol Sin* **30**, 673-680.

[58] Uteshev VV (2012) α7 nicotinic ACh receptors as a ligand-gated source of Ca(2+) ions: The search for a Ca(2+) optimum. *Adv Exp Med Biol* **740**, 603-638.

[59] Oz M, Ravindran A, Diaz-Ruiz O, Zhang L, Morales M (2003) The endogenous cannabinoid anandamide inhibits alpha7 nicotinic acetylcholine receptor-mediated responses in Xenopus oocytes. *J Pharmacol Exp Ther* **306**, 1003-1010.

[60] Butt C, Alptekin A, Shippenberg T, Oz M (2008) Endogenous cannabinoid anandamide inhibits nicotinic acetylcholine receptor function in mouse thalamic synaptosomes. *J Neurochem* **105**, 1235-1243.

[61] Twitchell W, Brown S, Mackie K (1997) Cannabinoids inhibit N- and P/Q-type calcium channels in cultured rat hippocampal neurons. *J Neurophysiol* **78**, 43-50.

[62] Wang HY, Stucky A, Liu J, Shen C, Trocme-Thibierge C, Morain P (2009) Dissociating beta-amyloid from alpha 7 nicotinic acetylcholine receptor by a novel therapeutic agent, S 24795, normalizes alpha 7 nicotinic acetylcholine and NMDA receptor function in Alzheimer's disease brain. *J Neurosci* **29**, 10961-10973.

[63] Tariot PN, Lopera F, Langbaum JB, Thomas RG, Hendrix S, Schneider LS, Rios-Romenets S, Giraldo M, Acosta N, Tobon C, Ramos C, Espinosa A, Cho W, Ward M, Clayton D, Friesenhahn M, Mackey H, Honigberg L, Sanabria Bohorquez S, Chen K, Walsh T, Langlois C, Reiman EM (2018) The Alzheimer's Prevention Initiative Autosomal-Dominant Alzheimer's Disease Trial: A study of crenezumab versus placebo in preclinical PSEN1 E280A mutation carriers to evaluate efficacy and safety in the treatment of autosomal-dominant Alzheimer's disease, including a placebo-treated noncarrier cohort. *Alzheimers Dement (N Y)* **4**, 150-160.

[64] Meilandt WJ, Maloney JA, Imperio J, Lalehzadeh G, Earr T, Crowell S, Bainbridge TW, Lu Y, Ernst JA, Fuji RN, Atwal JK (2019) Characterization of the selective *in vitro* and *in vivo* binding properties of crenezumab to oligomeric Aβ. *Alzheimers Res Ther* **11**, 97.

[65] Benek O, Korabecny J, Soukup O (2020) A perspective on multi-target drugs for Alzheimer's disease. *Trends Pharmacol Sci* **41**, 434-445.